Holocene Gypsum and Anhydrite of the Abu Dhabi Sabkha, Trucial Coast: an Alternative Explanation of Origin

Godfrey P. Butler
Esso Production Research Co
Post Office Box 2189
Houston, Texas

ABSTRACT

A holocene supratidal carbonate-algal stromatolite-evaporite cycle up to 3.7 m thick and underlying an area in excess of 100 km² occurs in the southeastern portion of the Trucial Coast, Arabian Gulf. Accumulation of evaporite facies is synchronous with development of oolite banks and coral reef growth in adjacent lagoons.

The diagenetic evaporite mineral assemblage includes gypsum, anhydrite and protodolomite. Components for these minerals have been derived from three sources: marine derived brines, continental groundwaters, and from exchange reactions between brines and host carbonate-evaporite sediment.

Calcium sulphate mineral genesis is in part primary precipitation from brines and in part a product of gypsum alteration, dolomitization and direct replacement of aragonite. Anhydrite is of secondary origin. Gypsum is the dominant source of components for anhydrite formation. The nodular texture of anhydrite results from an origin of anhydrite from gypsum.

Numerous structures in anhydrite (enterolithic seams, diapirs, and others) are described, some of which have been reported from ancient calcium sulphate sequences. These structures are diagnostic of anhydrite accumulation within a supratidal environment.

INTRODUCTION

The origin of large volumes of calcium sulphate minerals and the nature of the depositional environment has long been a puzzle. Theories of their origin have been greatly influenced by the 'basin evaporite' model of King (1942) and others. ever, more and more investigators of ancient e rite sequences (for example, Shearman, Fuller and Porter, 1969) are now concludin the depositional environment was supratida similar to that of sabkha deposits found along the Trucial Coast, Arabian Gulf. Many attributes of ancient evaporite sequences no quately explained by the 'basin evaporite' are resolved with the supratidal flat model intriguing possibility arises that many ancient orite sequences, particularly the sulphates, ac lated within a weathering profile of a supr flat. Shearman (1966) has gone so far as to pr that ancient supratidal evaporite sequences ar ert zone analogues of Coal Measure.

This paper describes a supratidal sabkha a the Trucial Coast that is extensively underla Holocene diagenetic gypsum ($CaSO_4 \cdot 2H_2O$ anhydrite ($CaSO_4$). Although the primary e sis of this paper is on the origin of gypsur anhydrite and the hydrologic environment, c structures in the evaporites are described v where found in ancient deposits, may provide tional support for genesis of the ancient depo a supratidal environment.

The material presented in this paper is the of eight months spent in the Trucial Coast and 1967). A detailed investigation of the str phy of one sabkha area, behind the island o Dhabi, was accomplished by digging trenche gering, and by probing. Samples of brine we lected from water collected in pits an squeezing the sediment. Most of the basi chemical data used in this paper are repor Butler (1969a).

TRUCIAL COAST ENVIRONMENT

Regional setting.

The Trucial Coast is located in the southeastern part of the Arabian Gulf and stretches from just to the east of Abu Dhabi Island to the Sabkha Mutti in the west (Fig. 1). The Trucial Coast comprises a number of shallow water carbonate and supratidal evaporite environments. Waters of the Arabian Gulf shoal gradually into a coast line of barrier islands and shallow lagoons, which in turn shoal into a low lying broad coastal plain which is terminated by low hills of older rocks and sand dunes on the continental margin.

The lagoon barrier island sediments consist of oolite deltas at lagoon entrances, with coral reefs and skeletal sands in the drainage channels and in front of the islands. The sediments of the mid-and inner-lagoon areas include quartz sands, skeletal sands, pelleted sands and aragonite muds, with local development of mangroves and algal mats. The muds, mangroves and algal mats are restricted to the shallow, low energy environments in the lee of small islands and in shoal areas. Many of the inner-lagoon shores are characterized by growth of algal mats up to 2 km wide (Kendall and Skipwith, 1968). The algal mats pass back into the flats of the coastal plain without break in slope.

These flats are known as sabkhas. Sabkha (with a variety of spellings) is a term frequently used in Arab countries to describe salt flats or salt marshes. Sabkhas are developed along the entire coastline, a distance of almost 500 kms. In the east, the flats are broad and continue apart from a few isolated hills of Tertiary and Quaternary rock (jebels) which project up above the surface. In the west, however, the flats are separated into a series of isolated pockets opening to seaward by ridges of older rocks which reach the coast as headlands. In their widest part, the coastal sabkhas are almost 40 km wide. To the south, they are bordered almost everywhere by a low escarpment of older rocks. Exceptionally, as in the east, the coastal sabkhas grade imperceptibly into inland or continental sabkhas (Fig. 1).

The sediment of the Holocene sabkhas include: carbonate sediment similar to that presently forming in the lagoons, recycled Pleistocene aeolianites and detrital Miocene silts and clays, shell concentrates and shell sands of beach ridges, and wind-blown detritus. Except for fringing shoreline areas, carbonate sediments dominantly underlie only one sabkha area south of Abu Dhabi Island (herein called the Abu Dhabi sabkha) (Fig. 1).

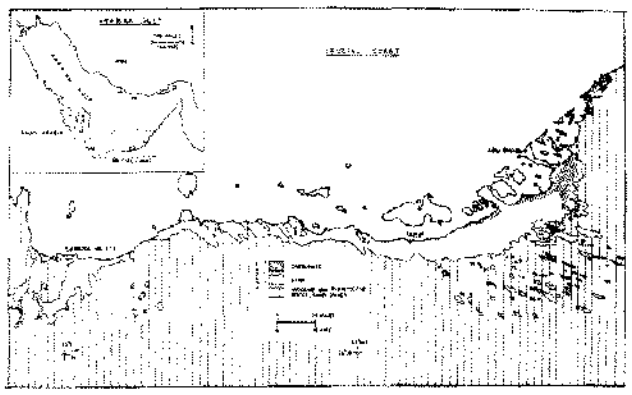

Figure 1. Trucial Coast and area of coastal sabkha. Area indicated "sand" is predominantly beach ridges.

The sabkha sediments are host to a variety of evaporite minerals. Contrary to the reported distribution of evaporites along the Trucial Coast (Kinsman, 1964, 1966; Evans and others, 1965), the bulk of the diagenetic evaporite minerals (gypsum, anhydrite and protodolomite amongst others) are restricted to the Abu Dhabi sabkha. Gypsum and anhydrite do occur in the detrital sediments of other sabkha areas along the Trucial Coast, but they are patchily distributed and nowhere do they achieve the areal development and the thickness as in the Abu Dhabi sabkha.

The Holocene sabkha sediments along the Trucial Coast are accumulating on rocks of Miocene and Pleistocene age. The Miocene rocks consist of a sequence of marls, sandstones, limestones and evaporites. Banked up against these rocks and covering them are rocks of Quaternary age which occur as two distinct lithologic units. The lower unit consists of a massive to small-scale trough bedded, locally loosely cemented calcareous sand (frosted and angular quartz grains, carbonate grains and feldspar) with a high miliolid content. It is probably of aeolin origin. The unit attains its greatest thickness in the area of the Abu Dhabi sabkha from which it thins to the east and to the west. The upper unit is a well-cemented, coarse, shelly carbonate sand with localized coral development (Kendall and Skipwith, 1969).

The Pleistocene rocks have been deeply eroded, and the upper unit is localized to jebel caps and to the escarpment. Where the lower aeolian sand unit is exposed under the skin of Holocene sediments, it frequently shows the morphology of a wave cut platform particularly along the base of the

escarpment and around jebels. The escarpment probably represented a Pleistocene shoreline with the jebels as offshore stacks.

Origin of the Trucial Coast sabkha.

The marine regression which has led to the evolution of the coastal sabkha plane may have been caused either by a relative fall in sea level, by a process of depositional regression, or by a combination of these processes.

Evans and others (1964) attributed the evolution of the sabkha as a process of depositional regression caused by intertidal sedimentation and to growth of beach ridges from headlands and knolls of older rock with no change in sea level. This view has also been expressed by other works in the Trucial Coast (Kinsman, 1964, 1966; Shearman, 1966; Butler, 1965; and Kendall and Skipwith, 1969). This process of depositional regression has been compared with that operating in the English Wash (Evans, 1965), the Chenier Plain of Louisiana (Price, 1955), and the flats of the Colorado Delta in the Gulf of California (Walker and Thompson, 1968).

Recently, there has been evidence to suggest that a Recent fall in sea level has caused the outward growth of the sabkha. Kinsman (1969a) tentatively concluded from the tracing of subsurface algal layers in leveled profiles across the Abu Dhabi sabkha, that there has been a "relative fall of sea level of 5-6 feet over the past 3-4000 years." The presence of coral in Upper Pleistocene carbonate rocks now elevated above present sea level, and the visually slightly elevated wave-cut platforms in trough-bedded Lower Pleistocene aeolianites at the base of the jebels and at the inland sabkha margin, are consistent with a relative fall in sea level in Recent time.

ABU DHABI ENVIRONMENT

The Abu Dhabi area is located toward the eastern end of the Trucial Coast (Fig. 1) and comprises three major geomorphic units: the islands, the shoal and channel areas (lagoons), and the coastal sabkha (Fig. 2).

Islands.

The islands (Abu Dhabi, Saydat, and others) are underlain by Miocene and Pleistocene rocks. They are low lying, and the older rocks are covered locally with sand dunes and beach ridges. Coral reefs occur just offshore of the island of Abu Dhabi. Protected shoreline areas in the lee of the islands

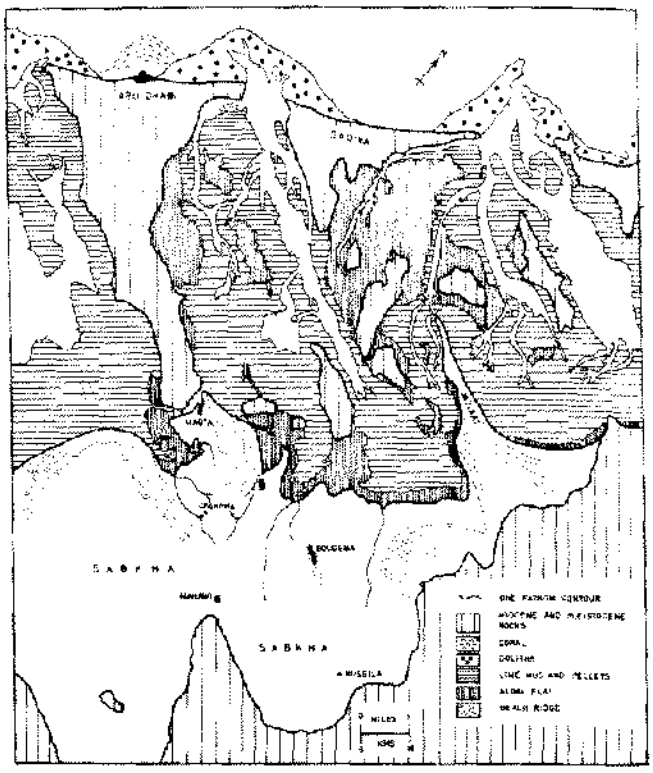

Figure 2. Interpreted lithofacies distribution in Abu Dhabi area.

are sites of accumulation of pelleted and fine grained argonite muds, mangroves and algal mats.

Shoal and channel areas.

The shoal and channel areas are flanked by the major islands. The waters are rarely 1 m deep except in tidal channels where depth may exceed 4 m. It is a large area of carbonate shoals fed and drained by a series of sub-parallel drainage channels. These channels are essentially feeders to large axial channels. Ebb deltas of oolites occur at the mouths of these axial channels. A platform of Pleistocene aeolianites underlies most of the area, and small remnants of it project up to form islands. Around these small islands carbonate sediments and skeletal sands have accumulated, and algal mats are common in protected areas. Much of the shoal and channel areas are intertidal and are sites of mangrove growth and algal mat development. Salinities of lagoon waters seldom exceed 80 ‰ and calcium sulphate and other more soluble evaporite minerals are absent.

Coastal sabkha.

The Abu Dhabi coastal sabkha has an area of approximately 200 km^2. The easterly portion of

this sabkha, to the east of Maqta and Mahawi has an area in excess of 100 km^2 and at its broadest part is 13 km wide. This sabkha is terminated further to the east by a shelf of Pleistocene rock, which projects out into the shoal and channel area at Jazirat (Fig. 2). The seaward margin of the Abu Dhabi sabkha is bordered by algal flats and at the landward margin by low hills (20 m high) of Miocene and Pleistocene rock which form an embayment.

Shoreline regression rates along the Trucial Coast are in the order of 1-2 m per year (Kinsman, 1969b). The shoal and channel areas in the Abu Dhabi area are at most 24 km wide. Thus within the next 12-24,000 years, the total width of the coastal sabkha could be in the order of 40 km.

Stratigraphy.

In the Abu Dhabi sabkha, the Quaternary sediments are in the order of 12 m thick and overlie a basement of Miocene rocks. These sediments are made up of approximately 9 m of Pleistocene aeolianites and up to 2.7 m of Holocene lagoonal, infratidal and intertidal carbonate and algal sediments. The overlying supratidal sediments range in thickness from almost zero to about 1 m (Fig. 3).

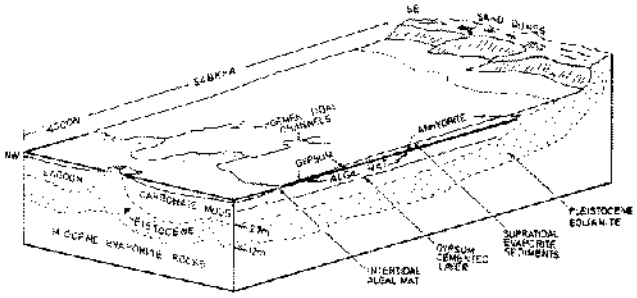

Figure 3. Stratigraphy and morphology of Abu Dhabi area (Schematic).

Sediments of the lower intertidal zone consist of aragonite muds, which pass back into extensive algal mats of the upper intertidal zone. These mats extend along almost the entire coastline in the Abu Dhabi area, and are up to 0.8 km wide. Growth of algae appears to be determined by the frequency and duration of subaerial exposure and salinity of tidal waters (Kendall and Skipwith, 1968). The algal mats trap carbonate sediment and are preserved below the surface as stromalitic laminae up to 0.6 m thick.

The present upper intertidal algal mats are laterally continuous with a subsurface algal mat in the sabkha interior. The areal distribution of subsurface algal mat, which also defines the areas of sabkha underlain by carbonate sediments, emphasizes that the Holocene sediments accumulated in two shallow basins within the underlying Pleistocene aeolianite (Fig. 4). These sands crop out around and in the lee of Bougeba and Maqta and within a broad zone at the landward sabkha margin (Fig. 4).

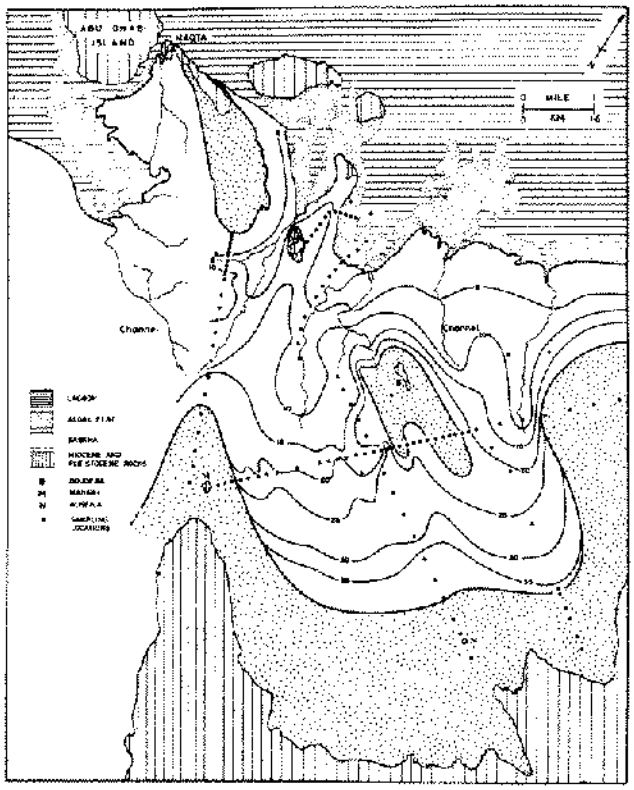

Figure 4. Distribution of Pleistocene aeolianite and depth of algal mat relative to uncontrolled surface elevation. C.I. = 5 in.

The carbonate sediments in the sabkha are similar to those presently accumulating in the shoal and channel areas to seaward. In the sabkha, uncemented, water saturated aeolianites in the subsurface pass up into a series of coarse sandy skeletal carbonates, fine grained carbonate muds which are capped with a layer of stromatolitic algal laminae. This algal layer is in turn overlain by a sequency of aragonite muds (locally protodolomitic) with algal filiments, and recycled aeolianites.

These supratidal sediments are host to gypsum, anhydrite and halite and other evaporite minerals of minor occurrence. Diagenetic gypsum and protodolomite also occur within the algal sediments and the underlying carbonate muds.

Thin cemented layers of varying degrees of hardness occur at various depths throughout the carbonate, underlying the algal sediments. These layers are generally not laterally continuous, with the exception of one layer at an almost constant depth of approximately 1.9 m relative to the sabkha surface in the mid-sabkha region and about 60 cm depth in the seaward sabkha margin. This layer is approximately 6 cm thick and consists of sediment grains and shell fragments cemented with gypsum. This layer is probably a continuation of an aragonite cemented layer found in the subsurface of the inner-lagoon carbonate muds (Kendall and Skipwith, 1969). These cemented layers play a major role in the restriction of groundwater movement within the sabkha sediments.

Geomorphology.

Over much of the sabkha the surface appears to be planar and it is estimated that the surface has an overall slope towards the sea of between 1/1000 and 1/2000 (00°02' and 00°03'). Locally, the smooth surface is interrupted by isolated jebels of older rocks (Maqta, Mahawi, Bougeba and Nueisla, Fig. 2), by platforms of Pleistocene rock, by depressions, and by low beach ridges. The depressions, which are elongate are oriented roughly normal to the coastline, coincide with the axes of former lagoon tidal channels (Fig. 2). Platforms of Pleistocene rock underlie the area to the extreme east of the Abu Dhabi sabkha, south of Maqta, in the environs of Bougeba and at the landward margin of the sabkha. Small remnants of the platforms project up above the surface as jebels. These areas of platform are commonly covered with a skin of deflated beach ridges.

The surface sediments are pale reddish brown in color and are composed of recycled Pleistocene aeolianite, shell sands and locally banks of shells. The coarser deposits occur around jebels and at the landward margin of the sabkha.

Over large areas the surface is blistered and encrusted with salt, and polygonal cracks are common. Blistering of the surface is excessive in areas bordering the hills at the sabkha margin. Elsewhere the surface is relatively smooth and only slightly encrusted with salt.

A number of processes have contributed to the development of the surface. The dominant process is considered to be flooding by seawater swept in during times of high winds from the northwest and/or during storms. These floodwaters dissolve halite crusts, and rework, and to some extent redistribute, the surface sediments. Wind also plays a role in adding dust, and locally deflating the surface. Evidence for deflation is shown by perched debris such as pieces of wood, bottles and beetles; blown out sides of surface polygons; and exposed gypsum crystals and anhydrite nodules. Aeolian erosion is particularly obvious in the relatively dry, slightly elevated areas of the surface of beach ridges and around jebels. In other parts of the sabkha the deflationary processes are probably arrested when the zone of capillary wetting is reached. These processes are actively infilling hollows and degrading slightly elevated areas of surface and will ultimately lead to a surface of greater equilibrium.

Climate and temperature.

The Trucial Coast environment is hot and extremely arid. Air temperatures range annually from 16°C to 44°C, and relative humidity varies between 90 percent during the night to 30 percent during the day. Average rainfall is 3.8 cm over the following time span:

Year	Rainfall (cm)	Highest individual fall (cm)
1958	2.87	1.37
1959	6.73	2.44
1960	2.67	1.53
1961	1.70	1.04
1962	0.33	0.30
1963	5.99	2.59
1964 (Jan)	5.66	1.98

Evaporation rates along the Trucial Coast are estimated to be as much as 124 cm per year (Privett, 1959), compared with a value of 260 cm for a similar evaporite forming environment on Bonaire, Dutch Antilles (Deffeyes and others, 1965) and 140 cm along the west coast of Baja California, Mexico (Phleger and Ewing, 1962).

Temperatures at the sabkha surface showed a maximum diurnal range of 15° to 53°C (February to May, 1964 and 1967). The highest surface temperatures were recorded in the seaward margin of

the sabkha where maximum temperatures were generally 8°C higher than elsewhere over the sabkha.

Analysis of a large number of temperature profiles within the sabkha sediments from February to May (1964, 1967) suggest that diurnal temperature fluctuations tend to die out within the upper 30 cm of sediment. Furthermore, at a depth of 50 cm the average temperature at the end of February was approximately 25°C, this increasing to approximately 28°C at the end of March. Apparently, temperature varies by about 3°C per month at this depth. Assuming that there is an orderly temperature variation over the year, the average maximum annual temperature range at 50 cm depth is calculated at 22°C to 40°C, averaging around 31°C, with the maximum temperature of 40°C occurring between July and August.

These temperatures appear reasonably accurate since 39°C groundwater temperatures recorded for July and August (Kinsman, 1964) compared favorably with a calculated temperature of 40°C and 35°C recorded temperatures for October and November (Curtis and others, 1963) compare favorably with a calculated temperature of 31°C. The temperature data also suggest that the effect of the annual temperature variation within the sediments extends down to the subsurface Pleistocene sand boundary at an approximate depth of 2.7 m, where temperatures of 30.5°C were recorded in April, 1967.

Physiochemistry and hydrology.

As a consequence of conditions of high net evaporation in the sabkha environment, fluids interstitial to the sediments are highly concentrated. Concentration of fluids has resulted in the separation of some of the major ionic components as gypsum and halite. The total thickness of calcium sulphate alone, however, exceeds 0.5 m. Theoretically, such a thickness of calcium sulphate would require the evaporation of a column of sea water 1,250 m high. Thus it is unlikely that the observed thickness of calcium sulphate could have formed from original fluids left in the sediments during the withdrawal of the sea. Furthermore, presence of free water within 1 m of the surface indicates that the fluids are abundant in the sediments. It was thought initially that water loss by evaporation was partly made up by the subsurface flow of brines through the sediments from the lagoons (Kinsman, 1966; Shearman, 1966). Kinsman (1964, 1966) further considered from unspecified mass balance estimations that extensive reflux occurred of dense brines back to the lagoons.

Contrary to these views held by other workers in the Trucial Coast, observations by the writer, together with an understanding of the characteristics of the chemistry of interstitial brines and groundwaters, suggest that fluids are supplied to the sediments from two sources: from lagoon waters and from mainland groundwaters (continental groundwaters). Addition of these fluids greatly modifies the pattern of sediment diagenesis which would be expected if diagenesis were solely due to residual fluids.

Observations extending over a total period of eight months indicate that the seaward portion of the sabkha is regularly flooded by lagoon waters. Flooding of the surface occurs during times of strong onshore winds and/or during storms. These sheets of water are 2 cm deep and because of the low elevation of this portion of the sabkha much of the water is retained and soaks down into the sediments; the remainder drains back into the lagoons. Surface layers of sediment are either closely or loosely cemented together with halite. Consequently, floodwaters dissolve halite as they sweep in across the surface. The term *flood recharge* has been suggested (Butler, 1969a) as being descriptive of this flooding process which in part rejuvenates near surface interstitial brines, by delivery and which in part removes the more soluble salts by surface drainage of waters back to the lagoons. The importance of flooding in supratidal areas to the formation of modern evaporites has also been recognized by Masson (1955), Holser (1966) and by Phleger (1969).

A series of belts approximately parallel to the inner boundary of the upper intertidal zone can be distinguished on the basis of flood frequency. There is a direct correlation between flood frequency, the assemblage of diagenetic evaporite minerals and the degree of dolomitization of carbonate sediment. Details of this correlation are given later, but of interest is the role of former lagoon tidal channels in flooding. These channels, oriented roughly normal to the shore line, form areas of relatively low elevation, with shallow water tables (Fig. 5). They extend back deep into the mid-sabkha region. These channels act as conduits for floodwater, and possibly seepage water, into the sabkha interior.

Brine chemistry.

Much of the chemical data presented will be elaborated in a later section, and only data

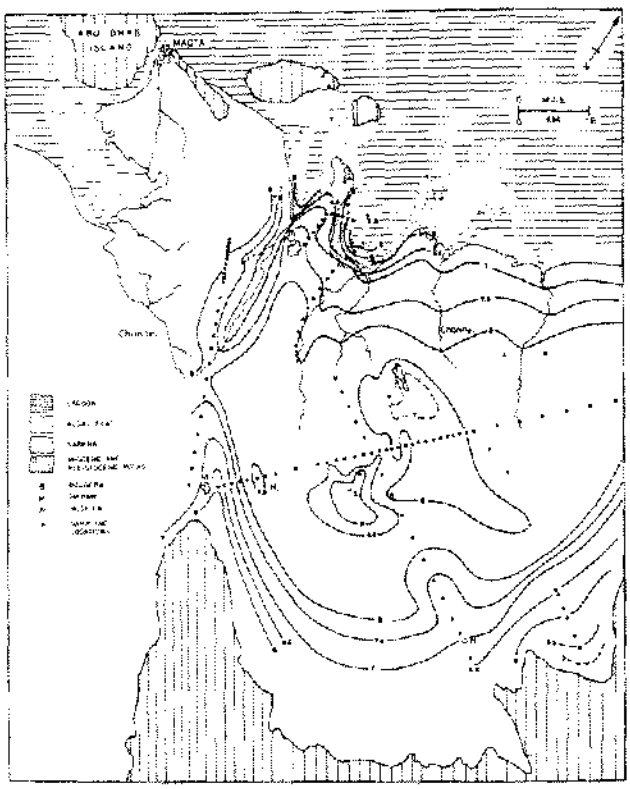

Figure 5. Depth to water table relative to uncontrolled surface elevation, C.I. = 5 in.

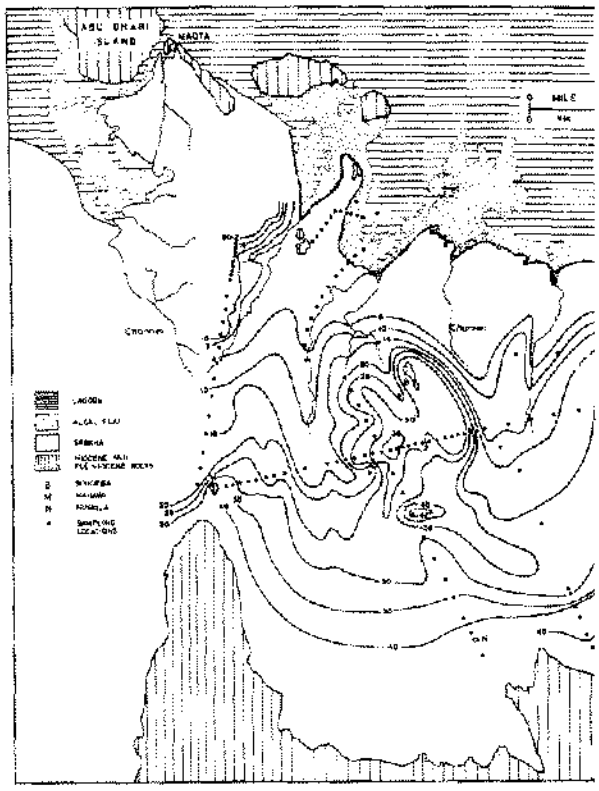

Figure 6. Concentration index of groundwaters. Areas H_1, H_2 of halite cementation. C.I. = x0.5.

applicable to the hydrology of the sabkha will be discussed here.

Brine concentration. For ease of reference, brine chlorinity is recast into a concentration index relative to standard seawater, by taking the ratio of measured brine chlorinity to a chlorinity of 19.35‰ of standard seawater. Thus, standard seawater has concentration x1.

Inner-lagoon waters have concentration x2.3 which rises to a plateau of between x8 and x9 in the mid-sabkha region and then falls to x5.5 at the landward margin (Fig. 6). The mid-sabkha region near Bougeba is characterized by brines of relatively low concentration. Anomously high concentrations of brine occur at localities H_1 and H_2 (Fig. 6). Over most of the sabkha concentration decreases with depth from the surface except within a zone at the seaward margin where the concentration gradient increases with depth (Fig. 7).

Groundwaters on the mainland and on Abu Dhabi Island are either potable or very brackish. Well waters around, and to the south of Tarif (Fig. 1) contain between 1 and 80 parts per thousand (ppt) total dissolved solids, and the Abu Dl Town well water used for drinking contains 8 total dissolved solids compared with 35 pp standard seawater. Evans (persenal communica 1967) found water of about normal seawater centration at depth in aeolianites at the inl sabkha margin 20 km south of Mahawi. These suggest that the Pleistocene aeolianites act as a ervoir for waters of low concentration.

It would be expected that concentration sabkha brines would be highest at the inland gin because these brines would be older than th to seaward. Furthermore, concentration ough uniformly decrease towards the sea. Therefo appears from the data presented that brines in seaward portion of the sabkha were derived f lagoon waters and brines in the inland por from continental groundwaters. Similarly, brines of relatively low concentration to the sc and east of Bougeba are also considered der from continental groundwaters.

There is evidence to suggest vertical influ brines derived from continental groundwater

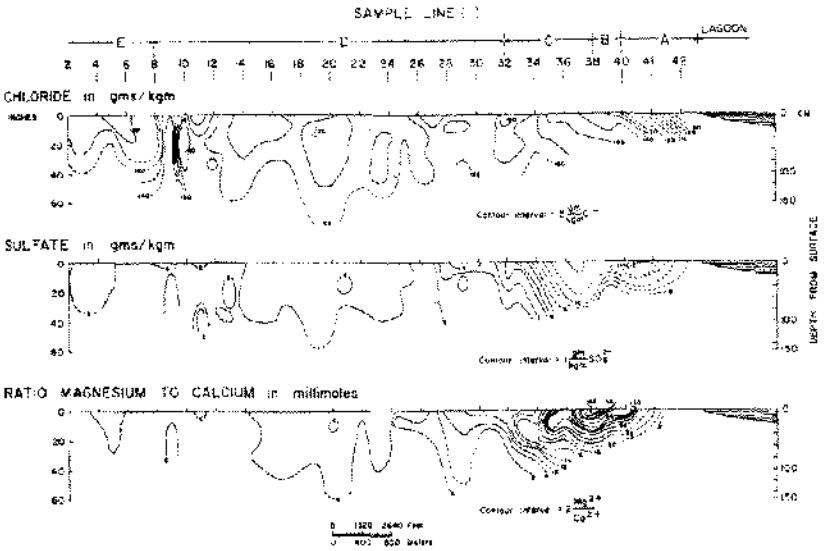

Figure 7. Vertical variation of Cl, SO_4 and Mg/Ca ratio across the sabkha (location of sample line 1: Butler, 1969a, Fig. 3). A to D = Facies 1 to 5 respectively.

the carbonate sediments in the mid–sabkha region. The configuration of lines of iso-concentration at Station 9 (Fig. 7) just to the west of Nuesila is consistent with the introduction of fluids of relatively low concentration from depth. Sediments at this locality are characteristically cemented with halite. Halite cementation of sediments to a depth of about 1 m also occur at localities H_1 and H_2 and correspond to the areas of anomolously high concentrated brines in the mid-sabkha region (Fig. 6). Thus, brines at these localities are also considered to be derived initially from continental groundwaters. The lack of other such localities in the sabkha with characteristics indicative of vertical influx of brines from depth suggests that the subsurface gypsum cemented layer in the carbonate unit acts as a seal and generally prevents movement to the surface of continental groundwaters from the subsurface Pleistocene sand aquifer. It is noted that in the localities where the sediments are cemented with halite, the gypsum cemented layer is locally absent. This layer has probably formed as a result of the interaction between pre-existing more concentrated fluids and less concentrated continental groundwaters moving up from the underlying aeolian sands.

In the seaward portion of the sabkha lines of equal concentration are deflected inland along the axes of former lagoon tidal channels. This configuration would result from the introduction of relatively less concentrated brines along these channels. Brine concentration is thus consistent with the flood recharge model.

Aerial distribution of pH, Mg/Ca ratio, and sulphate (SO_4) concentration in groundwaters, and distribution with depth of SO_4, Mg/Ca ratios, and pH are also found to be consistent with two sources of water in the sabkha and with the flood recharge process.

Brine pH. Inner-lagoon waters have pH 7.8 which decreases to 6.0 in the mid-sabkha and then rises again to 7.2 at the landward margin (Fig. 8).

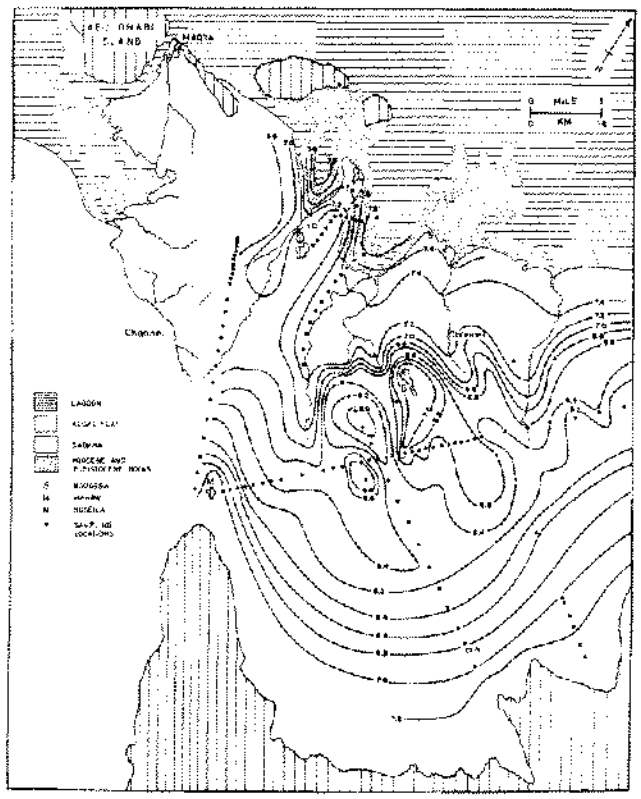

Figure 8. Groundwater pH. C.I. = 0.2 pH.

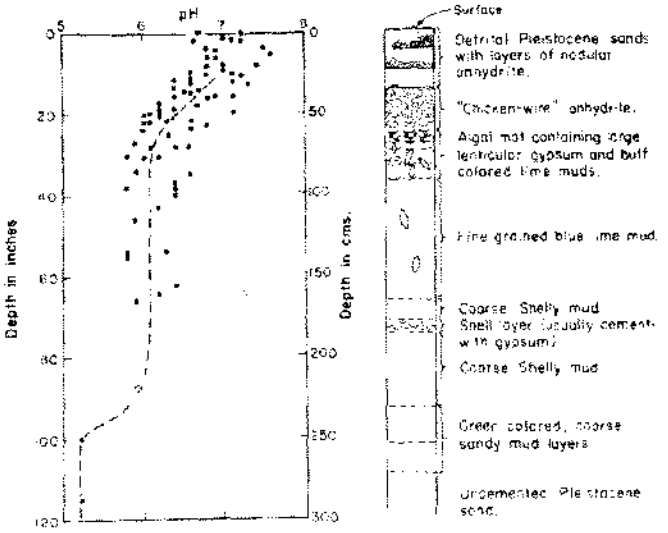

Figure 9. Accumulated profiles of interstitial fluid pH in Facies 4.

In the mid-sabkha region pH is seen to decrease with depth from the surface. Near surface fluids have an average pH of 7 which falls to pH 6 at 75 cm depth and pH 5.3 at a depth of 2.7 m at the base of the carbonate unit, and within the aeolian sands (Fig. 9).

Brine pH has evolved by a complex series of processes which include the effects of organic decomposition and mixing of marine derived brines with brines derived from continental groundwaters. Progressive concentration of fluids by evaporation would normally result in alkaline values of pH because of the decreasing solubility of CO_2. Thus a number of processes must have operated to reduce pH of sabkha brines to low levels (~pH 5-6). The carbonate sediments contain a very large percentage of organic matter, and its subsequent decomposition probably plays a major role in determining pH. That extensive organic decomposition does occur is suggested by the composition of gas in the sediments, which compared with air contains a high proportion of CO_2, CH_4, and H_2S:

Sabkha gas (mol percent)		air (mol percent)
N_2	94.99	79.9
O_2	4.76	20.0
CO_2	0.19	0.03
CH_4	0.06	–
H_2S	0.01	–

The activity of micro-organism is a function of the pH and Eh of the environment (Wood, 1962). Values of Eh recorded in the carbonate sediments in the mid-sabkha region were greater than - 200 mv, which fixes the pH to approximately 6 for the viability of common reducing microorganisms (Wood, 1962). This approximately agrees with the minimum observed fluid pH in the carbonate sediments of the mid-sabkha region (Fig. 9). Thus the relatively low values of pH (5.3) toward the base of the carbonate unit, and within the underlying aeolian sands, are probably not due to organic agencies.

Water wells to the south of Tarif have pH in the range of 5.2 to 8.7. Thus influx of fluids of variable pH could account for low values of pH in the sabkha subsurface, and the relatively high values at the inland sabkha margin and around Bougeba. Progressive decrease of pH towards the mid-sabkha from the inland margin could consequently be attributed to the result of mixing of the continental derived brines with brines affected by organic decomposition. It is noteworthy that if subsurface brines of low pH are the result of influx of continental groundwaters, then the vertical pH profile shown in Figure 9 would suggest that there is generally very little vertical mixing of continental groundwaters with preexisting fluids below a depth of about 1.7 m. This again suggests that the subsurface gypsum layer arrests vertical movement of groundwaters.

Magnesium to calcium ratio. The aerial distribution of values of Mg/Ca in groundwaters is shown in Figure 10. Inner-lagoon waters have values of about 5.3 which is approximately that found in standard seawater. Across the sabkha, values rapidly increase from 5.3 to a maximum of about 38, and then progressively fall to about 3 at the inland margin. Values decrease with depth from the surface with the highest gradients occurring within a zone at the seaward sabkha margin (Fig. 7).

The increase in Mg/Ca values reflects progressive depletion of Ca from the brines with increasing concentration, by precipitation of aragonite and gypsum; subsequent decrease in the values is attributed to dolomitization of carbonate sediment.

From Figure 10 it is seen that in a configuration similar to that of contours of concentration and pH, lines of iso-Mg/Ca ratio are deflected inland along channel axes, and relatively low values occur in the vicinity of Bougeba and at the inland margin. The deflection of lines of iso-Mg/Ca values along channel axes is further evidence for the flood recharge process.

Comparison between the distribution of aeolian sands in the sabkha (Fig. 4) and distribution of relatively low values of Mg/Ca, indicate that boundaries are generally concurrent. Dolomite does not occur in these sands and thus brines with

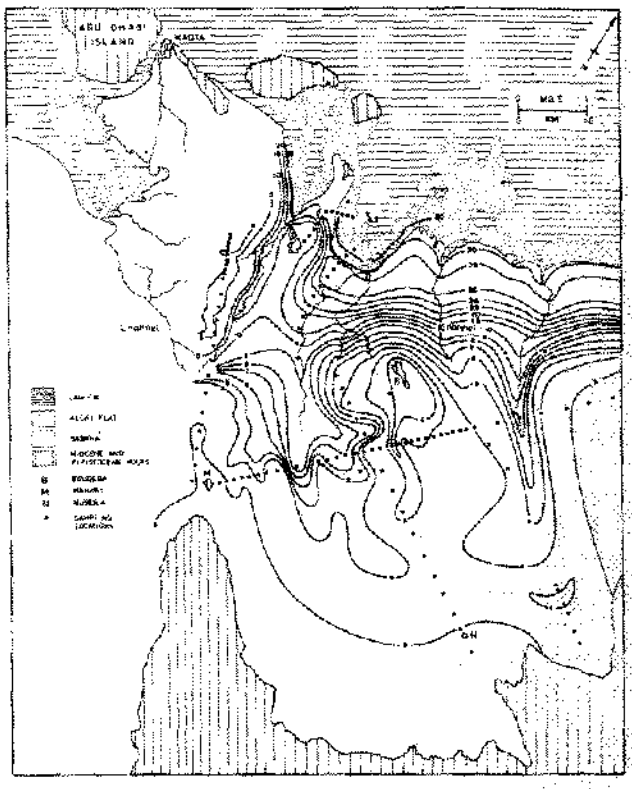

Figure 10. Mg/Ca (moi) ratio in groundwaters. C.I. = unity from 3 to 10; 5 from 10 to 35.

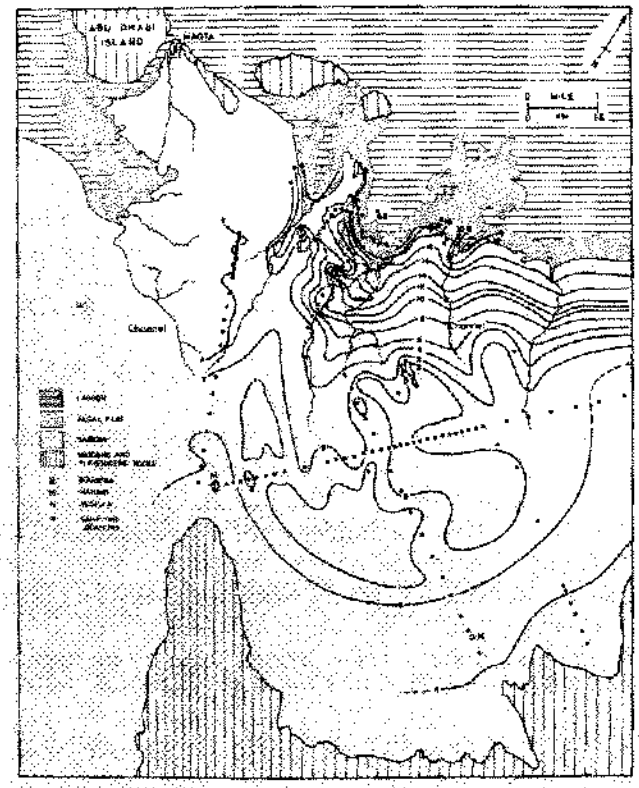

Figure 11. Sulphate concentration (gm/kg) in groundwaters. C.I. = 1 and 2, subsequent interval = 2.

relatively low Mg/Ca values of 2 to 3 are considered to be of continental origin. Support for this argument is found in the composition of water in wells in the environs of Tarif and from Abu Dhabi Island. These waters have values of Mg/Ca which range from 0.2 to about 0.8. Slightly higher values observed in the sabkha could be incurred by mixing of continental derived brines with residual brines in the sediments and/or by precipitation of Ca as gypsum.

Sulphate concentration. Inner-lagoon waters contain 6.3 gm per kg SO_4, a content which ranges upward to values in excess of 16 within a narrow zone at the seaward margin of the sabkha. Further inland values progressively decrease to less than 1 in the mid-sabkha and then rise to greater than 4 towards the inland sabkha margin (Fig. 11). With depth, SO_4 generally decreases, with the steepest gradients occurring within the narrow zone at the seaward margin. This also coincides with lateral boundaries of the greatest vertical and lateral variation in the Mg/Ca ratios (Figs. 7, 10).

It is evident from comparison of concentration (Fig. 6) and Mg/Ca values (Fig. 10) with SO_4 values (Fig. 11) in the mid-sabkha to the south and east of Bougeba and at localities H_1 and H_2, that similar anomalies occur in these parameters. Brines are either of relatively low concentration, high SO_4, and low Mg/Ca as around Bougeba, or of relatively high concentration, low SO_4, and high Mg/Ca as at localities H_1 and H_2. These anomalies are attributed to the initial low concentration of continental groundwaters and to local effects of brine mixing and precipitation of gypsum.

Finally, the landward depression of iso-SO_4 lines along channel axes is consistent with brines of relatively low concentration, and thus relatively high SO_4, introduced by surface floodwaters into the sabkha interior.

Diagenetic implications of hydrology.

On the assumption that diagenesis was solely due to residual connate fluids, processes would be quickly terminated for the lack of components; diagenetic patterns would be relatively simple and degree of sediment alteration would be fairly uniform throughout the sabkha. But because the

sabkha system is not closed with regard to the input of fluids, normal patterns of diagenesis are distorted, and the sequence of diagenetic events are made complex, particularly with respect to the relatively slow process of dolomitization.

Variation in brine chemistry in the sediments results in two gross diagenetic environments: a marine environment confined to the seaward portion or the sabkha (generally restricted to the upper 1.7 m of sediment) and a continental environment confined to the landward portion of the sabkha (restricted to the deeper sabkha subsurface, except where these fluids locally gain access to the surface of spread laterally in the carbonate sediments above the gypsum cemented layer, as at the landward margin and to the south and east of Bougeba). This dichotomy of environments is probably dynamic in nature. In the past when the sabkha was smaller, brines were dominantly of marine origin; but with gradual seaward accretion of sediments, these marine brines have been superceded by an overlay of brines derived from continental groundwaters. Thus two broad overlapping diagenetic fronts can be visualized as moving to seaward as belts with the progressive broading of the sabkha. Sediment diagenesis through marine brines is subsequently appreciable modified by input of other-source components.

It is apparent from the chemical data presented that fluids of accredited continental origin in the sabkha are either more, or less concentrated, than the surrounding fluids. The more concentrated brines have probably evolved by mixing and isolation from surrounding fluids by decrease in sediment permeability as a result of halite cementation. In brines of initial seawater composition solubility of gypsum decreases with increasing ionic strength of solution (Posjnak, 1940). Thus separation of gypsum from these highly concentrated brines would account for the relatively low concentrations of SO_4 and relatively high values of Mg/Ca. In contrast, brines which spread out to the south and east of Bougeba from the aeolian sands initially are relatively less concentrated than surrounding brines and thus contain more SO_4 (2gm per km) and have lower values of Mg/Ca (2 to 3) compared with the surrounding brines (SO_4 = < 1gm per kg; Mg/Ca=4). Thus these brines are potentially capable of further dolomitization of carbonate sediment and also precipitating gypsum with evaporation and/or mixing with the more concentrated surrounding brines. Influx of these brines probably accounts for structures observed in anhydrite seams, these structures generally restricted in the sabkha to two areas: just to the south and east of Bougeba, and within a zone parallel to the embayment hills just seaward of Nuseila. Anhydrite structures also occur at Station 9 (Fig. 7) and at localities H_1 and H_2 (Fig. 6).

The movement of water onto the sabkha by the flood recharge process also plays a major, though superficial role, in the accumulation and distribution of diagenetic evaporite minerals. Flood recharge prevents excessive accumulation of halite and more soluble bittern salts by dissolution and partial return of components back to the lagoons. Floodwaters also add to near surface fluids components for additional gypsum accumulation, and partly tops up the reservoir of magnesium ions depleted in the dolomitization of carbonates. The role of former lagoon tidal channels in the sabkha and flood recharge in dolomitization is illustrated by contours of the Mg/Ca ratio in brines along channel axes. The Mg/Ca = 5 for example is depressed far back into the mid-sabkha region (Fig. 10). Thus Mg ions (and other brine components) are not only kept supplied to older sabkha areas but are selectively supplied to well defined areas. This is supported by analysis of aragonite muds overlying the subsurface algal mats in channel areas and in areas bordering the channels. Channel muds contain ~ 80 percent protodolomite whereas the carbonate along the channel borders contain up to 10 percent protodolomite.

The most active areas of sediment diagenesis appears to be restricted to a zone at the seaward margin of the sabkha, as is indicated by the greatest lateral and vertical variation of the Mg/Ca ratios and SO_4 concentrations (Figs. 7, 10, 11). Thus in addition to the two described diagenetic belts, there is a third belt at the seaward sabkha margin, which moves out with the progressive broadening of the sabkha.

Kinsman (1966) proposed that reflux of dense brines through the subsurface back to the lagoons was operating in the sabkha. The implied model was that proposed by King (1942) for shallow lagoons, and more recently by Deffeyes and others (1965) as operating in the salina and tidal flats of Bonaire. Data presented in this section does not appear consistent with an overall reflux of brines in the sabkha. Reflux was evoked as a mechanism to explain large scale dolomitization of carbonate sediments and the lack of thick halite deposits associated with less soluble evaporite minerals in the ancient evaporite rocks. It is evident that the flood recharge process operating in the sabkha serves the same purpose as the proposed reflux of brines.

DISTRIBUTION OF EVAPORITES

For purposes of description, supratidal sediments of the Abu Dhabi sabkha are subdivided into a number of facies to depict the correlation between the hydrologic regimes and diagenetic features developed (Fig. 12).

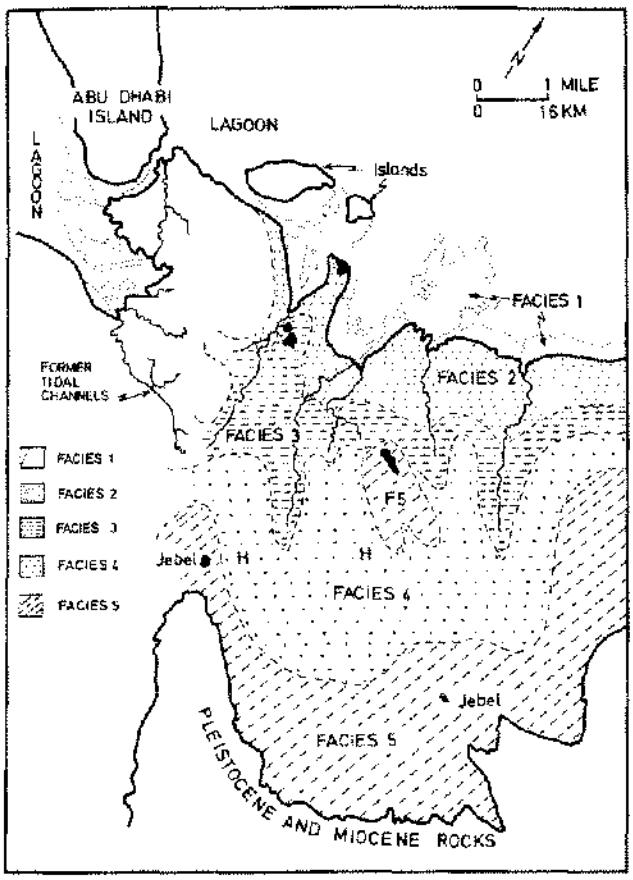

Figure 12. Distribution of evaporite facies. Areas H_1, H_2 sites of halite cementation.

Facies (1).

This facies coincides with the sedimentation and diagenesis in the upper intertidal zone. The zone, up to 0.8 km wide, is characterized by laminated mats of blue-green algae commonly interlayered with aragonite mud. The algal mats are underlain by lagoonal and lower intertidal aragonite muds. The zone is regularly flooded by tidal waters. Diagenetic processes include: (1) precipitation of aragonite; (2) precipitation of gypsum (crystals are < 1 mm long, lens shaped and flattened parallel to the c-axis); and (3) local cementation of surface sediments by aragonite, magnesite, and protodolomite to form crusts. The dolomitic crusts resemble those described by Shinn and others (1965) on Andros Island, Bahamas.

Facies (2).

This facies is characterized by a surface mush of displacement gypsum crystals (up to 2 cm long) which forms a zone up to 2.5 km wide. Anhydrite occurs at the surface of the mush towards the landward margin. Flooding occurs at monthly or less frequent intervals. The gypsum mush, which overlies a former upper intertidal algal mat, is up to 30 cm thick and on the basis of associated sediment can be subdivided into two horizons. In the lower horizon the gypsum crystals are associated with aragonite muds and algal filiments; in the upper horizon gypsum crystals are growing in recycled aeolianite and some early diagenetic aragonite. Diagenetic features include: (1) interstitial precipitation of aragonite, (2) gypsum precipitation, (3) solution of gypsum, (4) local surface alteration of gypsum to anhydrite via bassinite, and (5) local resolution of anhydrite. Camel and human footprints are commonly underlain by surface casts of anhydrite.

Facies (3).

Flooding of this zone, which is up to 1.6 km wide, occurs at less than monthly intervals. It is a zone of transition between Facies 2 and Facies 4. Diagenetic processes include: (1) partial replacement of preexisting gypsum mush by anhydrite, (2) precipitation of gypsum as crystals and as pore filling gypsum, (3) alteration of pore filling gypsum to anhydrite, (4) extensive local dolomitization (~ 80 percent) of aragonitic muds to form protodolomite in channel areas, and (5) solution of gypsum crystals.

Facies (4).

Flooding of this zone can occur as little as once every four to five years. The zone is up to 4.8 km wide. Sediment diagenesis is influenced by an overlap of the continental groundwater regime onto an earlier marine water regime.

The first six of the following diagenetic processes or features are considered due to the marine regime, the remainder to the additional effects of the continental regime:

(1) Complete alteration of an initial gypsum crystal mush to anhydrite, forming up to a 30 cm thick bed of chicken-wire anhydrite over an area approximately 10 km^2.

(2) Local alteration of small (⩽ 1 mm long) discoidal gypsum crystals to anhydrite nodules (⩽ 1 mm diameter), this occurring between the algal laminae of the subsurface algal mat.

(3) Abundant development of large (~ 6 cm, but occasionally up to 25 cm long) lenticular gypsum crystals (selenite) in the algal mat and former lagoonal sediment.

(4) Protodolomite is present only in trace amounts (~ 10 percent) except in the landward extension of former lagoonal tidal channels from Facies 3 where it can be up to 80 percent.

(5) Internal molds of gastropod shells in anhydrite (Fig. 13a).

(6) Local occurrence of hopper crystals (⩽ 6 cm^3) in near surface recycled Pleistocene aeolianites.

(7) Development of structures in anhydrite: ptygmatic folds, disharmonic folds (thrust folds), diapir-like structures.

(8) Local cementation of supratidal evaporite and algal mat sediments by pore filling halite and hopper crystals (⩽ 24 cm^3). Cementation occurs within circular of ellipsoidal plugs up to 150 m diameter and 1 m deep (see Fig. 12, locations "H").

Facies (5).

Lagoonal and algal mat sediments are absent in these zones. The zone at landward margin of the sabkha has a maximum width of approximately 3 km. Sediments are essentially continental in origin and consist of Pleistocene aeolianites overlain by up to 60 cm of recycled aeolianites, shell lag material, and bedded skeletal debris. These zones are not flooded by lagoon waters. The groundwater regime is now entirely continental. The diagenetic and sedimentary processes and features include:

(1) Occurrence of alternating seams (⩽ 5 cm thick) of anhydrite nodules and detrital sands forming sequences up to 2 m thick (Fig. 13b); thick seams of anhydrite nodules up to 2.4 thick (Fig. 13c).

(2) Alteration of nodules and nodular anhydrite seams to gypsum. Secondary gypsum crystals up to 10 cms long are flattened parallel to the a-c plane and are zoned with anhydrite laths.

(3) Interstitial precipitation of gypsum forming cemented sediment layers.

(4) Locally, traces of polyhalite and sylvite in surface halite crusts.

ORIGIN OF GYPSUM AND ANHYDRITE

The evaporite minerals developed in the sab include aragonite, gypsum, anhydrite, protod mite and halite. Except for anhydrite and dolon the mineral associations resemble that major gr of solid phases which initially separate from water subject to progressive evaporation (Usigli Stewart, 1963). Anhydrite and protodolomite flects either primary precipitation of these mine under conditions peculiar to the sabkha envi ment or replacement reactions between com nents of preexisting phases and associated bri Kinsman (1966) concluded that the anhydrite a primary mineral and that the protodolomite formed by reaction between aragonite sedime and brines. Wells (1962) suggested that s gypsum in Qatar could have formed as a product of dolomitization:

$$2CaCO_3 + Mg + SO_4 + 2H_2O = CaMg(CO_3)_2 + CaSO_4.2$$

A further problem concerns the origin of nodular texture of anhydrite in the sabkha. T texture is characteristic of many ancient calci sulphate sequences and has been attributed to placement of gypsum (Kerr and Thompson, 19 Murray and others, 1964) or to the deformatio gelatinous layers of loose anhydrite crystals (R and Byrne, 1961). More recently, (Rooney French, 1968) nodular texture has been attribu to the interstitial precipitation of anhydrite wit supratidal sediments, largely as a result of the c clusions of Kinsman (1966) for the origin of an drite in the Trucial Coast sabkhas.

Contrary to the conclusions of other worker the Trucial Coast, the writer has evidence cons ent with an origin for sabkha anhydrite as do nantly an alteration product of gyps Furthermore, anhydrite nodules are the result anhydrite genesis from gypsum. Some anhyd appears also to have formed as a product of a placement reaction between aragonite and br components. The evidence is summarized as lows:

Stratigraphic relationships.

The generalized distribution of carbonate-al evaporite facies across the sabkha is shown in ure 14. Wherever there is appreciable developm of an upper intertidal algal mat, a surface gyps crystal mush of variable thickness and width occ

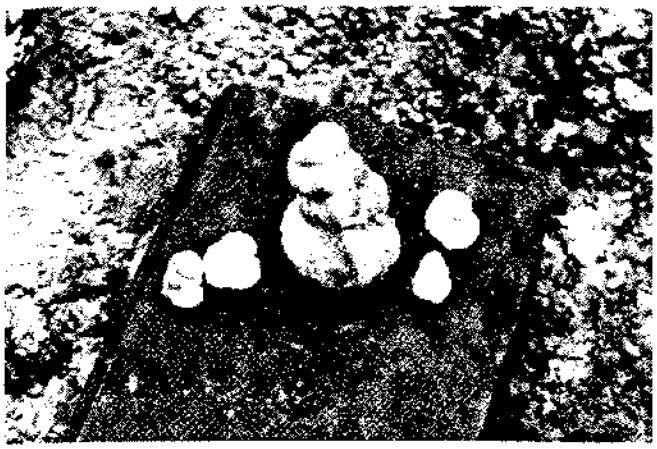

(a)

(c)

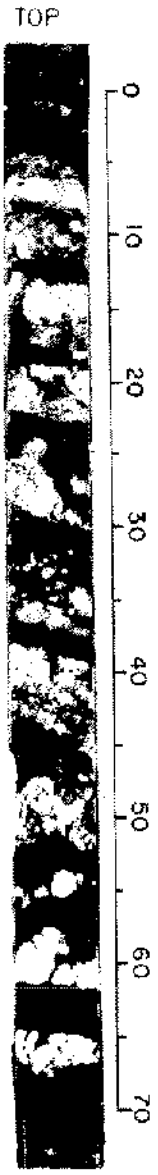

(b)

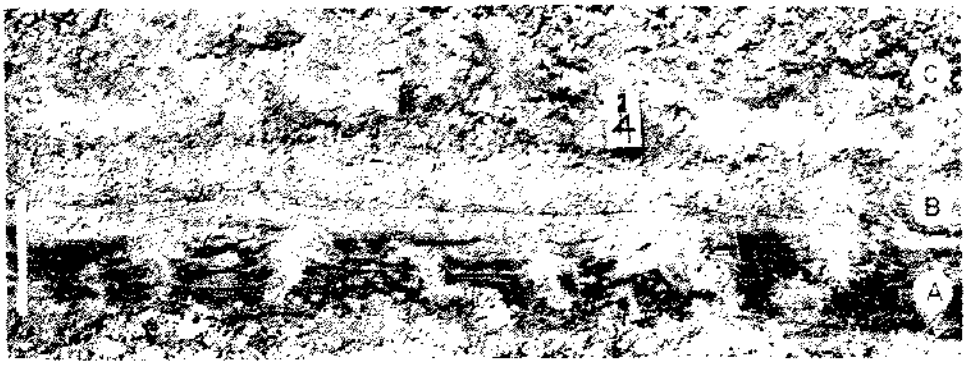

(d)

Figure 13. (a) Casts of gastropod shells in anhydrite. Height of center cast = 5 cm; (b) Core showing seams of anhydrite nodules, interlayered with acolianite. Scale in cm; (c) Trench wall showing upper portion of 2.4 m thick seam of anhydrite nodules in detrital Miocene silts and clays. Machete scale (left) = 0.6 m; (d) A = algal stromatolites, B = gypsum mush, C = recycled acolianite + anhydrite nodules. Scale = 20 cm.

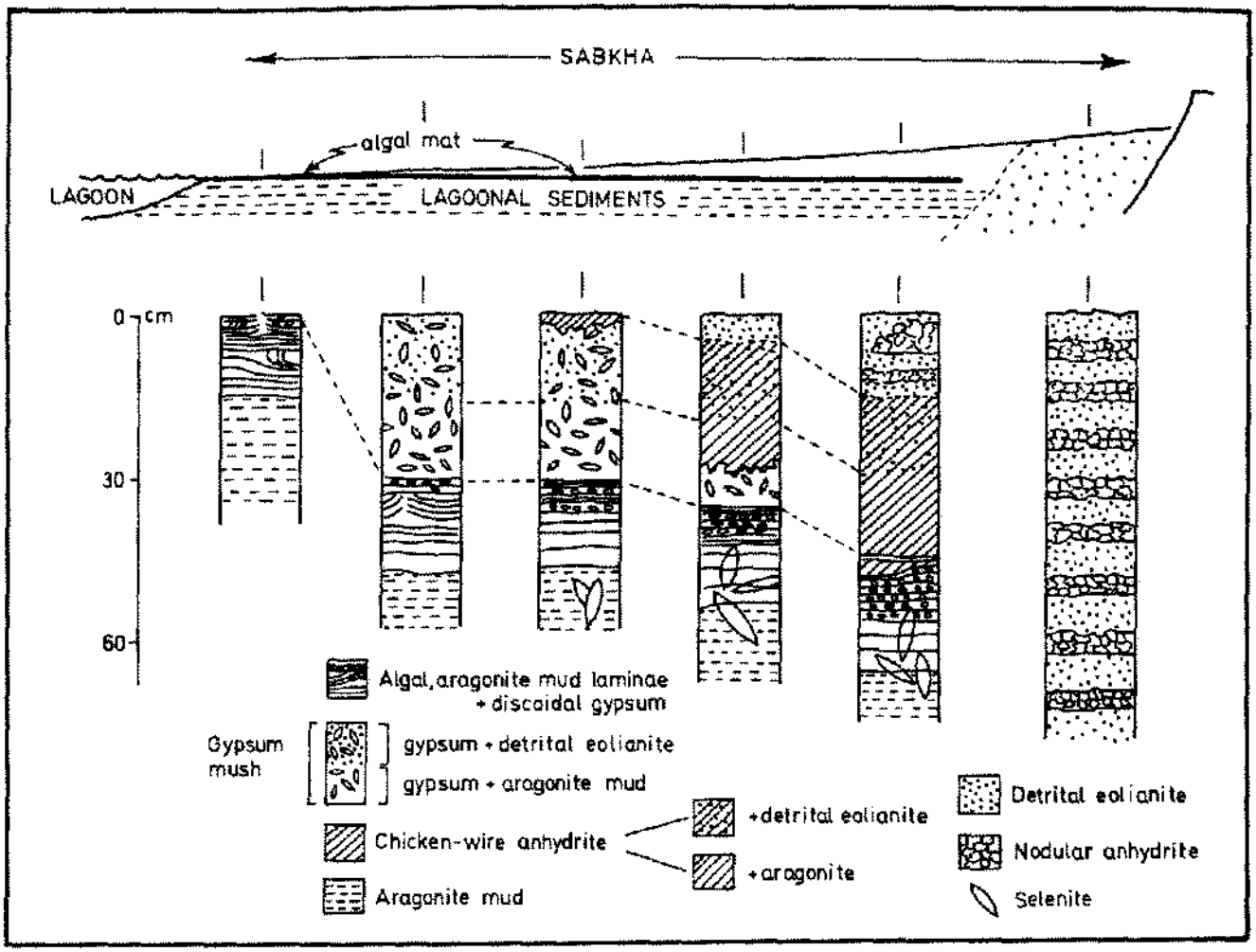

Figure 14. Vertical distribution of carbonate-algal-evaporite facies across sabkha.

just above the intertidal zone. Algal mats can be traced continuously in the sabkha subsurface over a distance of up to 9 km inland from the present upper intertidal algal mat (Fig. 13d). By analogy with the present distribution of algal mat and adjacent surface gypsum mush, it would be expected that the inland subsurface algal mat would also be overlain by a mush of gypsum crystals (Fig. 13d).

The present surface gypsum mush is up to 30 cm thick; and, as described previously, gypsum crystals in the lower half are supported in aragonite muds and algal filiments and in the upper half are supported in recycled aeolianite (Fig. 15a). In the mid-sabkha region (Facies 4) the subsurface algal mat is overlain by up to a 30 cm thick seam of chicken-wire anhydrite containing the same vertical distribution of sediments as observed in the gypsum mush to seaward. Trenches across the sabkha show the progressive replacement, from the top down, of a gypsum mush by anhydrite with a chicken-wire texture (Figs. 15a,b,c,d). This seam of chicken-wire anhydrite underlies an area in excess of 10 km^2. Pseudomorphs in anhydrite after discoidal gypsum crystals in the original mush were not observed.

Porosity (determined by neutron activation) of the gypsum mush ranges from 15 percent to 35 percent averaging 30 percent. The seam of secondary chicken-wire anhydrite, on the other hand, has an almost uniform porosity of approximately 20 percent (Fig. 16).

Locally within the mid-sabkha region, gypsum crystals ($\leqslant$ 2 mm long) within the algal laminations are replaced by anhydrite forming thin ($\leqslant$ 0.5 cm) alternating laminae of small ($\leqslant$ 2 mm) anhydrite nodules and organic layers up to 15 cm

(a)

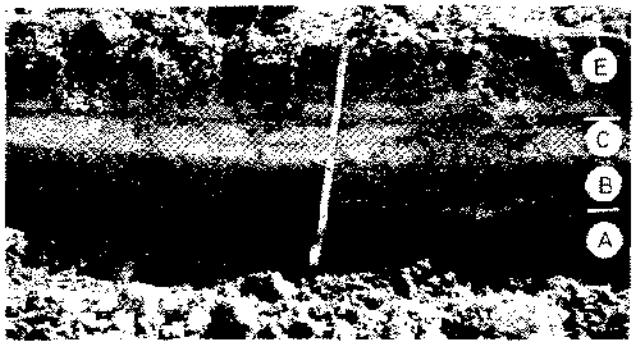

(b)

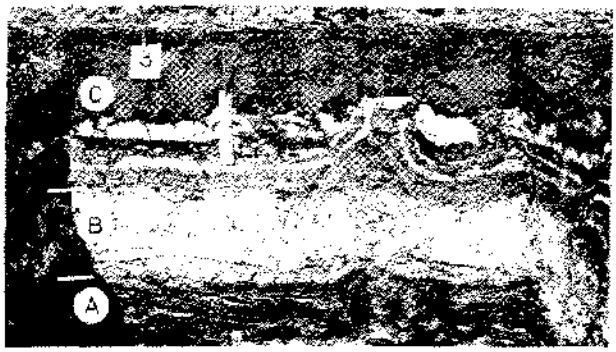

(c)

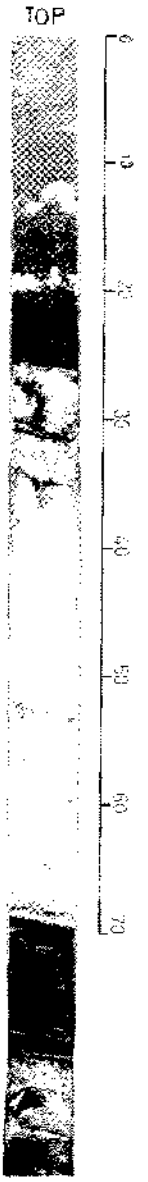

(d)

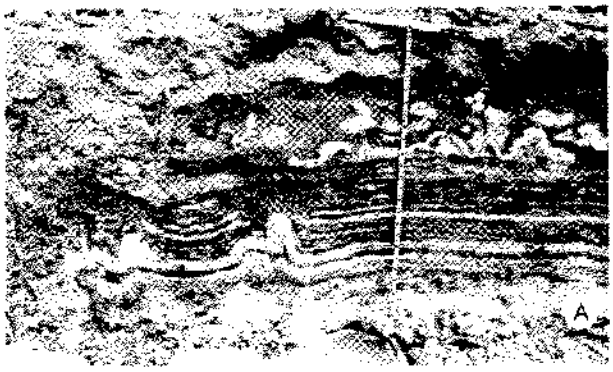

(e)

Figure 15. (a) Gypsum mush (B+C) in Facies 2. A = algae, B = gypsum + aragonite + algal filaments, C = gypsum + recycled aeolianite. Scale = 28 cm; (b) Partial alteration of gypsum mush (B+C) to anhydrite (Facies 3). A = algae, B = gypsum, C = anhydrite, E = recycled aeolianite. Scale = 12 in. (30 cm); (c) Complete alteration of original gypsum mush (B) to anhydrite (Facies 4). A = algae, B = anhydrite, C = recycled aeolianite = festooned anhydrite layers. Scale @ 15 cm; (d) Core showing details of the secondary anhydrite (35 cm to 70 cm) in (c). Above 50 cm = anhydrite nodules + recycled aeolianite. Below 50 cm = anhydrite nodules + aragonite; (e) Thin seams of nodular anhydrite in recycled aeolianite above secondary anhydrite seam (A). Note plications (center) and water table in (A). Exposed scale = 26 in (67 cm).

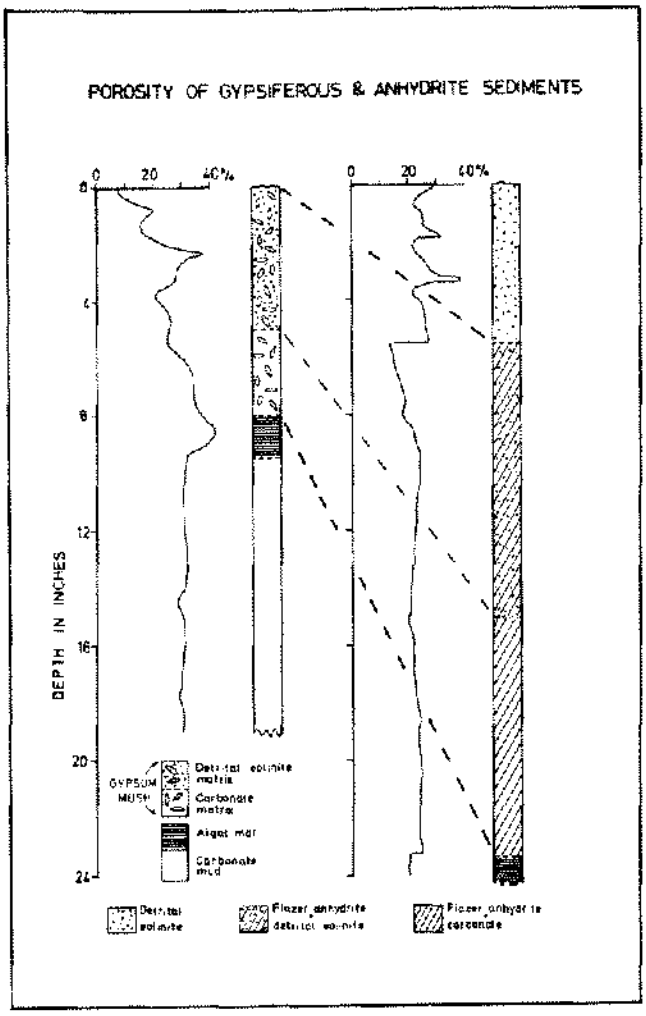

Figure 16.

thick. On compaction such laminae could easily resemble the familiar ancient varved anhydrites attributed to be of deep water origin. Furthermore, gypsum free aragonite-algal laminae couplets (2 mm to 4 mm thick) resemble some ancient bituminous dolomite/calcite laminates (Fuller and Porter, 1969, Fig. 12a, p. 919).

Again in the mid-sabkha region, the seam of secondary chicken-wire anhydrite is overlain by 30 cm to 60 cm of recycled aeolianite which contain thin (~ 0.5 cm to 3 cm thick) seams of nodular anhydrite, some of which show plications (Fig. 15e). These near surface nodular anhydrite seams postdate the seam of secondary chicken-wire anhydrite, and their origin can be explained on the basis of the flood recharge model. Inspection of the upper few centimeters of the sabkha surface in Facies 3, after the retreat of one of the flooding events, showed the entire surface affected by the floodwaters to contain small (~ 0.2 mm) discoidal and prismatic gypsum crystals. Analysis of these floodwaters showed a composition similar to brines at sodium chloride saturation from evaporating pans (see Fig. 19). The ionic strength of lagoon waters has subsequently been increased by solution of halite at the surface leading to the precipitation of Ca and SO_4 as gypsum. Subsequent burial of these gypsum crystals and alteration to anhydrite, together with repetition of the process with time, would yield the thin seams of anhydrite nodules observed in the mid-sabkha region. This reasoning may also be applied to explain the origin of seams of anhydrite nodules in the recycled and Pleistocene aeolianites at the landward margin of the sabkha (Fig. 13b).

Mechanism of gypsum dehydration to anhydrite.

Three mechanisms appear possible by which gypsum in contact with brines could dehydrate to anhydrite: (1) direct dehydration to anhydrite, (2) a solution-precipitation process, and (3) stepwise dehydration via intermediary bassinite.

Some gypsum crystals coexisting with anhydrite in Facies 2 and 3 are deeply eroded by solution. Solution cavities commonly have a rind of white, coarsely crystalline material. Commonly, such material also occurs inside crystals (Fig. 17a). X-ray analysis shows this material to be bassinite with traces of anhydrite and gypsum. Bassinite is similarly found associated with coexisting gypsum and anhydrite from Baja California. Apparently, alteration of some gypsum to anhydrite in the sabkha is a stepwise dehydration process. Hardie (1967) and Zen (1965) also conclude from solubility studies that sodium chloride solutions promote the stepwise dehydration process. Consideration of Sr/Ca ratios in gypsum and anhydrite, and Sr/Ca ratios in brines further suggests that a solution-precipitation process may also occur in the alteration of gypsum to anhydrite.

In localities where anhydrite has hydrated to gypsum, bassinite is not observed, this suggesting that the hydration process is simply one of solution-precipitation. As will be shown later, this conclusion is supported by strontium data.

Textural relationships.

Gypsum. On the basis of size, stratigraphic position and crystal habit, three types of gypsum crystals can be distinguished in the sediments.

Gypsum crystals generally restricted to the supratidal gypsum mush above the algal mat range in size from 0.1 mm to 2 cm in diameter and have a characteristic discoid shape with the plane of flattening approximately normal to the c-axis. Similar, though smaller (≤ 2 mm), crystals occur within the supratidal subsurface algal mat laminae. In the intertidal zone crystals are restricted to the upper few centimeters, but in the supratidal subsurface algal mat they locally occur within the upper 15 cm. The crystals are normally free from inclusions, but some very early diagenetic gypsum contains cores of aragonite. All gypsum crystals of these sizes and habit are of displacement origin.

Other larger (~ 4 cm to 30 cm diameter) crystals (selenite gypsum) with the plane of flattening also approximately normal to the c-axis, are restricted to the supratidal subsurface algal sediments and underlying carbonates. These selenite crystals are similar to those from the Laguna Madre described by Masson (1955). In some crystals host carbonate grains or algal layers are entrapped (Kinsman, 1966, Fig. 3a); in others, carbonate grains and shells and shell fragments are poikilitically enclosed. The close correlation between intra-algal laminae in selenite gypsum crystals and algal laminae in the surrounding algal-aragonite mud laminae, suggests that some of these crystals have developed, at least in part, by interstitial precipitation in algal sediment and in part by replacement of aragonite. Gastropod shells in selenite gypsum are sometimes partially or completely infilled with gypsum (see Lucia, 1968, p. 857, Fig. 23A for an example). This gypsum may locally be replaced by anhydrite (Fig. 13a). Shell fragments and aragonite mud may also be completely or partially replaced by gypsum, and thin sections of such material are similar to those shown by Illing and others (1964, p. 106, Figs. D, E, F).

In places there is evidence for resolution of selenite crystals as shown by serrated crystal edges and a relative decrease in crystal size compared with the original impression in the encasing sediment.

In channel areas in the mid-sabkha region, there is evidence for extensive solution of shells, and replacement of aragonite to form gypsum via the dolomitization process. In these areas, shells and shell fragments are very soft and easily ground to a paste between fingers. This suggests that the shell material has been extensively leached. The cations so supplied to the interstitial fluids may cause further precipitation of gypsum, either interstitially within the sediments or as an addition to preexisting gypsum crystals. In place in the channel areas, gypsum enclosed sediment which is almost totally dolomitized. The surrounding carbonate sediments contain little or no protodolomite. This strongly suggests that the gypsum has formed as a by-product of the dolomitization of aragonite. A similar mineral assemblage occurs in other places, but anhydrite is present rather than gypsum. Either the anhydrite has replaced secondary gypsum formed by dolomitization or anhydrite has been formed directly by dolomitization without intermediary gypsum. Textural relationships are indeterminate.

Finally, a third type of gypsum occurs in anhydrite, in association with celestite, within aeolian sands at the inland sabkha margin and just to the south and east of Bougeha. These gypsum crystals are flattened in the a-c plane and range from 0.5 cm up to 10 cm long. They are characteristically zoned with anhydrite laths, dust and small quartz grains. Anhydrite laths in the vicinity of these gypsum crystals have serrated edges indicative of solution. It is evident from the zonation and association of these gypsum crystals with anhydrite that they are of secondary origin and formed by hydration of anhydrite.

Anhydrite. Anhydrite in the sabkha has a dominantly nodular texture, although in some channel areas some anhydrite is without structure. Anhydrite nodules range from 0.05 mm to 30 cm in diameter. Larger nodules are commonly aggregates of smaller nodules. Nodular size is probably related to some extent to the size of the initial gypsum crystal: small nodules have formed from small crystals and large ones from large gypsum crystals. Solitary nodules are rare. More frequently nodules are aggregated to form seams of anhydrite of variable thickness. The thinnest seams are ~ 3 mm thick, the thickest 2.4 m thick.

Nodular shape is variable. Some are ellipsoidal with the longest dimension either horizontal or vertical. Others are almost spherical, pelleted, doughnut shaped (Fig. 17b), or have mammilated surfaces. Many small nodules have an enterolithic shape (Fig. 17c).

Internally, nodules are made up of anhydrite laths ranging in length from < to 100 mu. The arrangement of laths is typically felted, but a parallel or radial arrangement is not uncommon. In any single nodule the length of laths is variable, possibly reflecting several anhydrite generations.

Small nodules contain pelleted aragonite muds, foraminifera shells, and frosted and angular quartz grains. In larger nodules, these contaminants are conspicuously absent. It seems likely that during

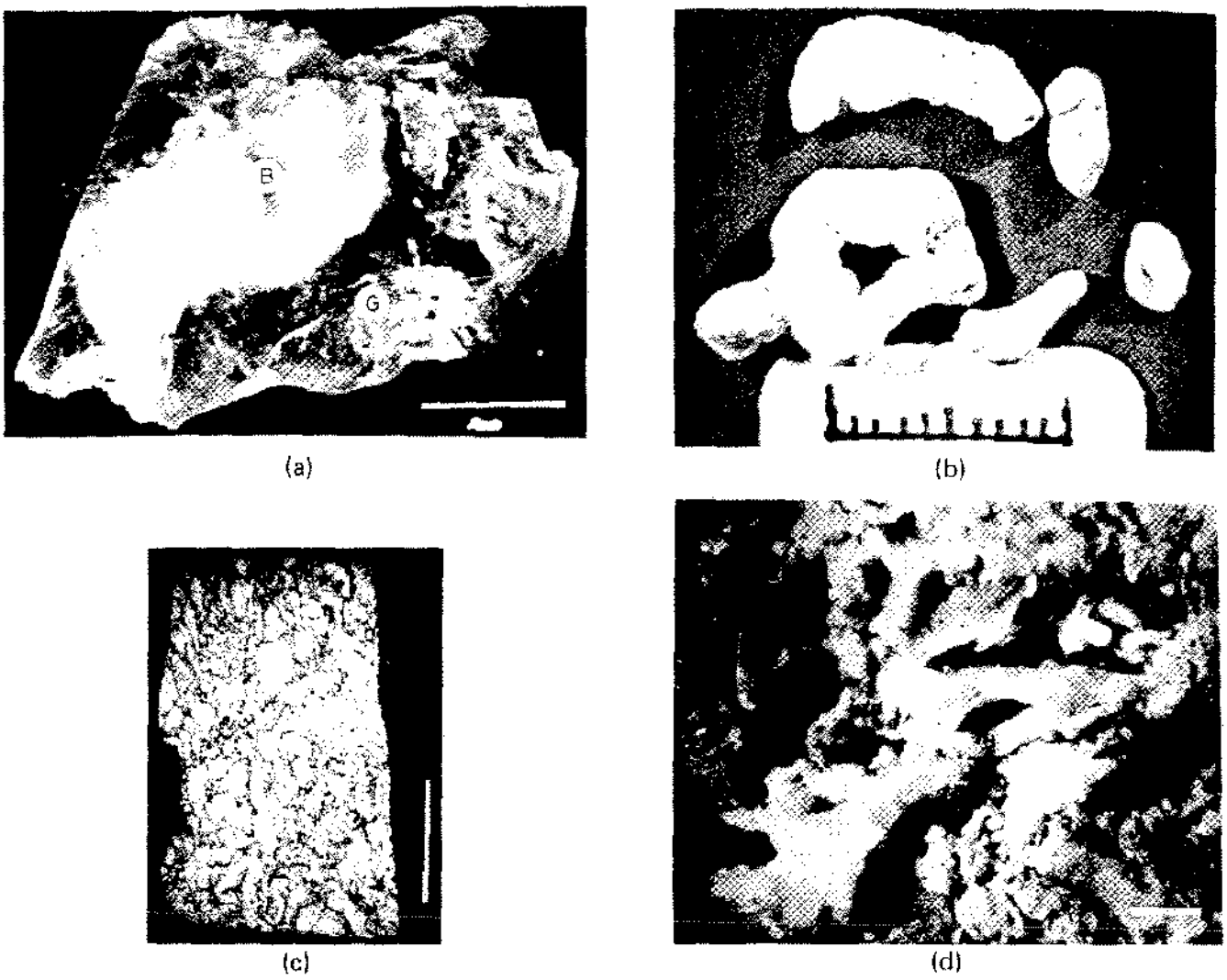

Figure 17. (a) Photomicrograph of a discoid gypsum crystal broken along cleavage. G = gypsum, B = bassinite. Scale = 1 mm; (b) Photomicrograph of anhydrite nodules from gypsum mush. Scale = 1 cm; (c) Photomicrograph of chicken-wire anhydrite. Note enterolithic "nodules," bottom and center. Host sediment is aragonite. Scale = 1 cm; (d) Photomicrograph of anhydrite pseudomorphs after discoid gypsum in groundmass of anhydrite. Scale = 2 mm.

the growth of nodules, shell, other carbonate particles and quartz grains, are forced to nodular boundaries, or some of the carbonate is replaced by anhydrite.

All seams of anhydrite nodules show the chicken-wire texture which is so characteristic of ancient nodular anhydrites. Nodules are generally separated by films of either aragonite or protodolomite-aragonite mud or aeolianite. In places in the aeolian sediments at the inland sabkha margin, well defined nodules are surrounded by anhydrite laths which are oriented with long axes tangential to nodular boundaries, thus forming a chicken-wire-like texture. This arrangement suggests a later generation of anhydrite.

One of Kinsman's (1966) major lines of argument for the primary origin of anhydrite was the apparent absence in the sabkha of anhydrite pseudomorphs after discoidal gypsum crystals. Although anhydrite pseudomorphs after gypsum have been recently recorded (Kinsman, 1969b, p. 884) within the upper 4 to 5 cm of coastal sabkha sediments in the seaward portion, this mechanism for anhydrite formation is not considered typical. The sabkha anhydrite is very fine grained, has the consistency of toothpaste, is thixotropic, and developed within loosely consolidated sediments. Pseudomorphs would not be expected to form in these sediments unless the alteration of gypsum to anhydrite is a process of direct dehydration, or the host matrix to gypsum crystals is sufficiently rigid to retain the shape of gypsum crystals during solution of gypsum and precipitation of anhydrite.

Anhydrite pseudomorphs after gypsum are rare

in the sabkha. In the writer's experience they are generally restricted to crystals exposed at the sediment surface in sandy areas and locally in the subsurface of channel areas. Dehydration of surface gypsum to anhydrite occurs via intermediary bassinite. Moiola and Glover (1965) recorded a similar mode of anhydrite formation from Clayton Playa, Nevada.

Shapes in anhydrite which are interpreted as anhydrite pseudomorphs after discoidal gypsum crystals occur locally in the subsurface of channel areas (Facies 3). The host anhydrite is typically non-nodular in hand specimen (Fig. 17d). Voids which have the characteristic shape of discoidal gypsum crystals are commonly associated with the anhydrite pseudomorphs. A series of parallel, closely spaced thin sections through a sample of this anhydrite suggests that these voids become progressively infilled with a later anhydrite. The potential pseudomorphic outlines are subsequently either obliterated or not visually apparent because of the resulting interlocking mesh of anhydrite laths at void boundaries. It is concluded that some anhydrite pseudomorphs after gypsum may form in restricted areas of the sabkha subsurface. Textures, however, suggest that the pseudomorphs dominantly originate by infilling of voids left by the solution of gypsum crystals in a sufficiently rigid host sediment; but conditions appear to be marginal for pseudomorph formation as well as preservation with later diagenesis. The bulk of the anhydrite nodules in the sabkha have *not* formed initially as pseudomorphs after gypsum.

Small anhydrite nodules in the subsurface gypsum mush in the seaward portion of the sabkha usually contain aragonite pellets. Anhydrite laths are commonly arranged radially to the surface of pellets, and occasionally small anhydrite laths are observed imbedded within the aragonite. Gypsum has not been observed to occur at pellet boundaries in association with the anhydrite. This may be taken to signify direct local dissolution of the aragonite with accompanying precipitation of anhydrite and without intermediary formation of gypsum.

Chemistry of brines.

Sampling and techniques of analysis of sabkha brines are reported in Butler (1969a). The variation of Ca, Mg and SO_4 concentrations with brine concentration across the sabkha are shown in Figure 18. These data may be compared with that of salt pan brines, Bahamas (Miller, 1961) (Fig. 19). It is of note that neither anhydrite nor dolomite were detected in the *in situ* brine pan precipitates.

Concentrations of Ca and SO_4 are essentially dependent on the solubility products of aragonite and gypsum/anhydrite with increasing brine concentration. If dolomitization occurs, then K_{sp} protodolomite will also partly control Ca and SO_4 concentrations. The chemical data (Fig. 18) suggest that a trace amount of Ca is crystallized as aragonite prior to the onset of gypsum precipitation at concentration $\times 3.4$ (65‰ Cl^-) within the intertidal zone. Across the supratidal area SO_4 is decreased by precipitation as gypsum/anhydrite. The continental derived brines at the landward margin of the sabkha also reflect gypsum/anhydrite precipitation. Seawater derived brines attain sodium chloride saturation at about concentration $\times 8$ (155‰ Cl^-) and specific gravity 1.20.

Concentration of SO_4 in the sabkha brines is reduced almost to zero at brine concentrations approaching sodium chloride saturation (Fig. 18). At a similar brine concentration in salt pan brines, approximately 20 m.mol/kg (40 m.eq./kg) of SO_4 remain after precipitation of almost all the Ca as carbonate and sulphate (Fig. 19). If the amount of SO_4 reduced to H_2S is insignificant the removal of the remaining SO_4 from the sabkha brines after the original Ca in solution has been utilized can only be realized through dolomitization or dissolution of aragonite.

Various authors have suggested a relationship between the dolomitization process ($2CaCO_3 + Mg = Ca\ Mg(CO_3)_2 + Ca$), and gypsum formation (von Morlot, 1848, *in* Cayeux 1935; Klement, 1895; Wells, 1962; and others). The composition of interstitial brines squeezed from various horizons in the sabkha sediment, together with the mineralogy of the host sediment is consistent with this hypothesis (Table 1, data *in* Butler, 1969a). The host sediment to all the deepest brine samples (Table 1) contained aragonite, protodolomite and gypsum: 39A contained algal mat and gypsum; 34C, aragonite and gypsum; 32A aragonite, protodolomite and anhydrite; and 29A, recycled aeolianite, anhydrite and aragonite.

The calculated addition of Ca ions to the deeper brine samples as a consequence of the aragonite-brine reaction and the subsequent adjustment of equilibration with SO_4 ions in the brine to form gypsum/anhydrite, compares remarkably well with the observed increase of Ca in the deeper brines.

In some sabkha areas, especially along channels, SO_4 removal as a consequence of dolomitization is probably the dominant mechanism. But in other areas, notably in the mid-sabkha region (Facies 4) where former tidal channels are absent, the upper-

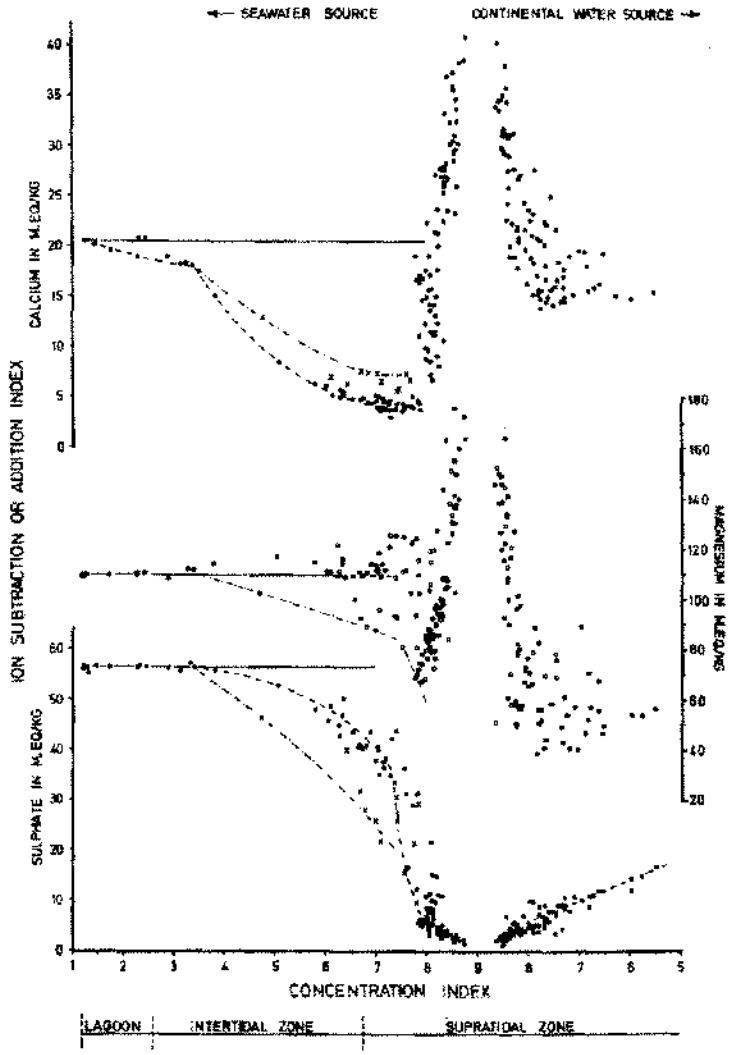

Figure 18. Concentration of ions in lagoon waters and interstitial sabkha brines. Ion subtraction or addition index = ratio of ion concentration to concentration index. Ca and SO_4 values designated 'x' indicate selected brines showing subtraction of Mg.

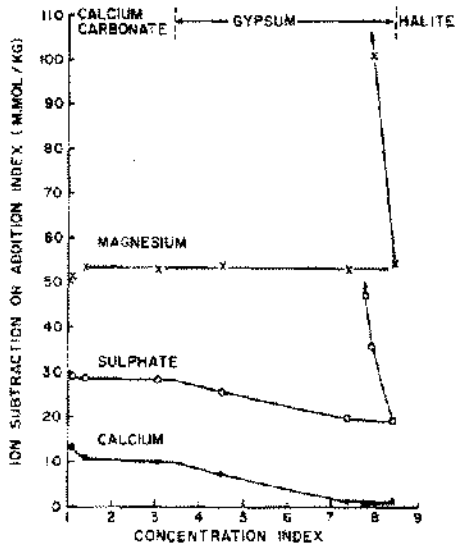

Figure 19. Composition of brines from evaporating pan, Bahamas. (Miller, 1961).

most lagoonal intertidal and supratidal carbonate sediments contain little or no protodolomite; gypsum and anhydrite are abundant; and interstitial fluids are almost depleted in SO_4. These data, together with the fact that interstitial brines are slightly acid (pH~6), are consistent with the addition of Ca to brines by aragonite dissolution followed by precipitation of gypsum/anhydrite. There is textural evidence, however, to tentatively suggest that anhydrite rather than gypsum may locally form as a consequence of aragonite dissolution and the dolomitization process.

In the seaward portion of the sabkha just inland of the intertidal zone, anhydrite first occurs associated with gypsum in brines of concentration approximately ×7.5. At the landward sabkha margin, secondary gypsum and anhydrite also coexist in brines of concentration approximately ×7.5 (Butler, 1965, 1969a). Consequently, these data suggest that anhydrite is the stable mineral in

Table 1. Quantitative Relationship Between Dolomitization and Gypsum Formation.

Station 39	Sample A Depth 13 cm	Sample B Depth 48 cm	Difference B–A
Cl^-	140.8	149.5	+8.7
Mg^{2+}	436	392	-44
SO_4^{2-}	125	82	-43
Ca^{2+}	13	19	+6

$$88CaCO_3 + 44\,Mg^{2+} + 43\,SO^{4\,2-} = 44\,Ca\,Mg\,(CO_3)_2 + 43\text{“}SO_4\text{”} + Ca^{2+}$$

Station 34	Sample B Depth 48 cm	Sample C Depth 71 cm	Difference C–B
Cl^-	157.0	160.9	+3.1
Mg^{2+}	481	445	-36
SO_4^{2-}	60	43	-17
Ca^{2+}	27	44	+17

$$72CaCO_3 + Mg^{2+} + 17\,SO_4^{2-} = 36Ca\,Mg(CO_3)_2 + 17\text{“}CaSO_4\text{”} + 19Ca^{2+}$$

Station 32	Sample A Depth 15 cm	Sample B Depth 67 cm	Difference B–A
Cl^-	146.3	151.2	+4.9
Mg^{2+}	303	265	-38
SO_4^{2-}	60	35	-25
Ca^{2+}	26	43	+17

$$76CaCO_3 + 38\,Mg^{2+} + 25\,SO_4^{2-} = 38Ca\,Mg(CO_3)_2 + 25\text{“}CaSO_4\text{”} + 13Ca^{2+}$$

Station 29	Sample A Depth 8 cm	Sample B Depth 22 cm	Difference B–A
Cl^-	154.3	158.0	+3.7
Mg^{2+}	339	321	-18
SO_4^{2-}	41	31	-10
Ca^{2+}	35	45	+10

$$36CaCO_3 + 18\,Mg^{2+}\ 10\ SO_4^{2-} = 18Ca\,Mg(CO_3)_2 + 10\text{“}CaSO_4\text{”} + 8Ca^{2+}$$

Cl^- in gm/kg; Mg^{2+}, SO_4^{2-}, Ca^{2+} in m. mol/kg.

brines of concentration $\geqslant \times 7.5$ ($\geqslant 145‰$ Cl). The calculated activities of water in brines coexisting with gypsum and anhydrite are in good agreement with the experimental data of Hardie (1967) and van't Hoff (1902, *in* Hardie, 1967) for gypsum-anhydrite equilibria (Fig. 20). The activities of water in sabkha brines were calculated using vapour pressure data of Arons and Kientzler (1954).

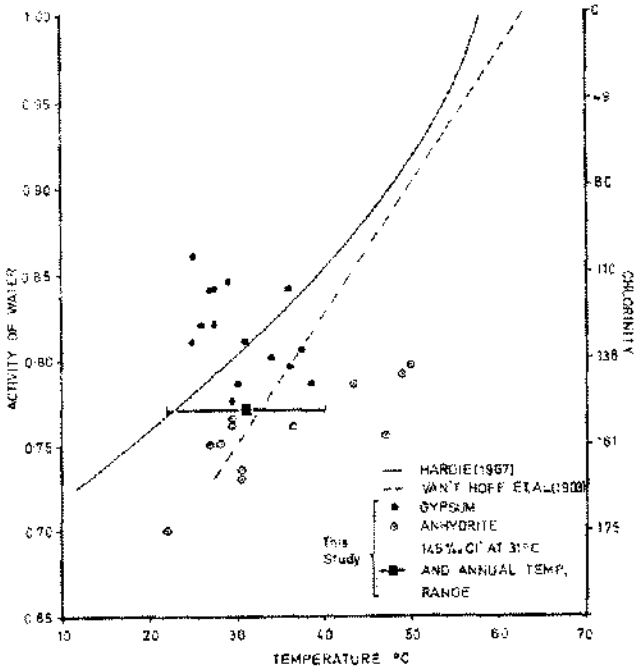

Figure 20. Activities of water in brines coexisting with gypsum and anhydrite.

Strontium.

One approach to an understanding of the origin of calcium sulphates in ancient evaporites has been to interpret their strontium contents. The interpretation of these data, however, has been largely based on speculation. For example, various authors (Phillips, 1947; Stewart, 1963) considered that primary anhydrite might contain more Sr than anhydrite which had replaced primary gypsum. The argument is based on the converse of the fact that gypsum which has replaced anhydrite by hydration contains less Sr than the parent anhydrite.

Interpretation of Sr concentrations in brines, aragonite, gypsum, anhydrite and protodolomite from the sabkha suggests that a tentative correlation can be made between Sr in brines, minerals precipitated and exchange of components between brines and host carbonate-evaporite sediments. Owing to the complexity involved in the interpretation of Sr data, only a summary will be presented here. A full treatment of the data will be presented elsewhere (Butler, 1969b).

The partial order of precipitation of minerals from evaporated seawater is aragonite, celestite and gypsum. Up to brine concentrations at which celestite and gypsum are crystallized, the Sr/Ca (mass fraction) ratio in brines would be controlled by the solubility product of aragonite, and the distribution coefficient k_{Sr} aragonite. At higher brine concentrations the Sr/Ca ratio in solution would be controlled by the solubility products of celestite, gypsum/anhydrite, and k_{Sr} gypsum/k_{Sr} anhydrite. If dolomitization takes place, k_{Sr} dolomite will also participate in the Sr budget. Knowledge of these variables will allow an estimation to be made of the Sr/Ca ratio in minerals precipitated from brines, with assumptions (among others) that equilibrium is maintained and that values for distribution coefficients remain constant with brine concentration. Values of distribution coefficients for some evaporite minerals are summarized as follows:

Mineral	k_{Sr}	Author
Aragonite	0.50	Kinsman and Holland (1969)
Gypsum	0.44	Purkayastha and Chatterjee (1966)
Anhydrite	0.51	Purkayastha and Chatterjee (1966)

Values of Sr calculated from the solubility of celestite in brines (Müller and Puchelt, 1961) parallels the trend of Sr concentrations in sabkha brines (Fig. 21). Strontium concentrations in sabkha brines are thus initially controlled by the solubility of celestite over the range in which gypsum or anhydrite are precipitated.

On the basis of known distribution coefficients and values of Sr/Ca ratios in brines of varying concentrations, values of Sr/Ca in minerals crystallized from these brines are calculated (Fig. 22). The Sr/Ca ratio in aragonite precipitated from lagoon waters ($\times 1.2$ to about $\times 2.3$) should have values ranging from about 19×10^{-3} to 9×10^{-3}. Similarly, in the concentration range $\times 3.35$ to $\times 7.5$, Sr/Ca (gypsum) should range from about 8×10^{-3} to 11×10^{-3}. Since anhydrite has been found to be stable in brines of concentrations $\geq \times 7.5$, Sr/Ca (anhydrite) should have a maximum value of 13×10^{-3} (Fig. 22). Prediction of values of Sr/Ca ratios in calcium sulphates crystallizing from brines of concentration $> \times 7.5$ is complicated by effects of NaCl saturation. But in these highly concentrated brines, the concentrations of Ca remain constant with continued progressive absolute brine concentration (Butler, 1969a, Fig. 8). Since the solubility of celestite always decreases with increasing brine concentration, values of Sr/Ca in brines should consequently decrease and Sr/Ca ratios in gypsum and anhydrite should consequently fall to values $<11\times10^{-3}$ and $<13\times10^{-3}$ respectively, by

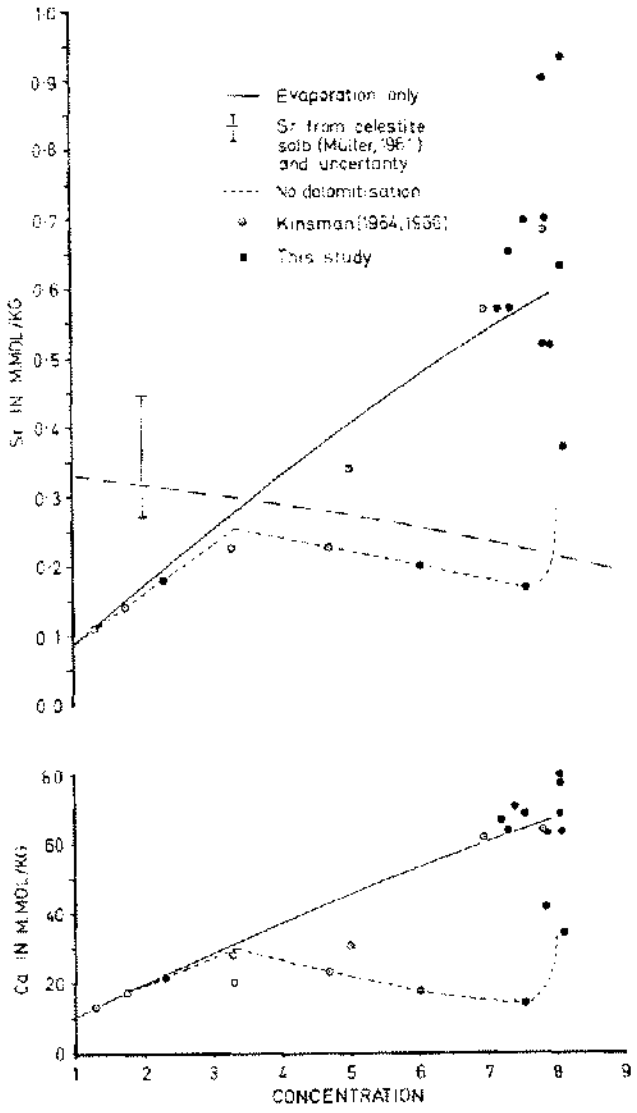

Figure 21. Sr and Ca in lagoon waters and sabkha brines.

precipitation from brines of concentrations $\geq \times 7.5$ (Fig. 22).

Strontium in evaporite minerals.

Aragonite. Two samples of aragonite from the sabkha contained 0.59 ± 0.004 wt percent Sr ($Sr/Ca = 13.2\times10^{-3}$) and 0.95 wt percent Sr ($Sr/Ca = 21.3\times10^{-3}$). In similar samples, Kinsman (1969b, p. 835) recorded a range of between 0.7 and 0.8 wt percent Sr ($Sr/Ca = 15.6\times10^{-3}$ to 17.9×10^{-3}) (Fig. 23). These values approximately agree with the expected range of Sr/Ca in aragonite precipitated from lagoon waters.

Gypsum. Discoidal gypsum crystals from the sabkha contained between 0.036 and 0.282 wt percent Sr ($Sr/Ca = 1.55\times10^{-3}$ to 12.2×10^{-3}) and selenite gypsum crystals 0.021 and 0.057 wt percent Sr ($Sr/Ca = 0.90\times10^{-3}$ to 2.46×10^{-3} (Fig. 23).

There is a direct correlation between the diameter of discoidal gypsum crystals and values of Sr/Ca. Small (<0.5mm diameter) crystals have high Sr/Ca ratios, which range from about 8×10^{-3} to 11×10^{-3}; larger crystals range between 5×10^{-3} and 3×10^{-3} (Fig. 24). Conversely, small gypsum crystals developed between algal laminae in the mid-sabkha region have Sr/Ca ratios similar to the large crystals in the surface gypsum mush.

Values of Sr/Ca ratios in the small discoidal gypsum crystals from the surface mush correlate with the predicted Sr/Ca of 8×10^{-3} to 11×10^{-3} for concentrations $\times 3.35$ to about $\times 7.5$. Furthermore, Müller (1962, p. 20) found that gypsum precipitated from a brine of concentration $\times 4$ had a Sr/Ca ratio of 9.5×10^{-3} and at $\times 5$, 11.2×10^{-3}. Consequently, small discoidal gypsum crystals from the

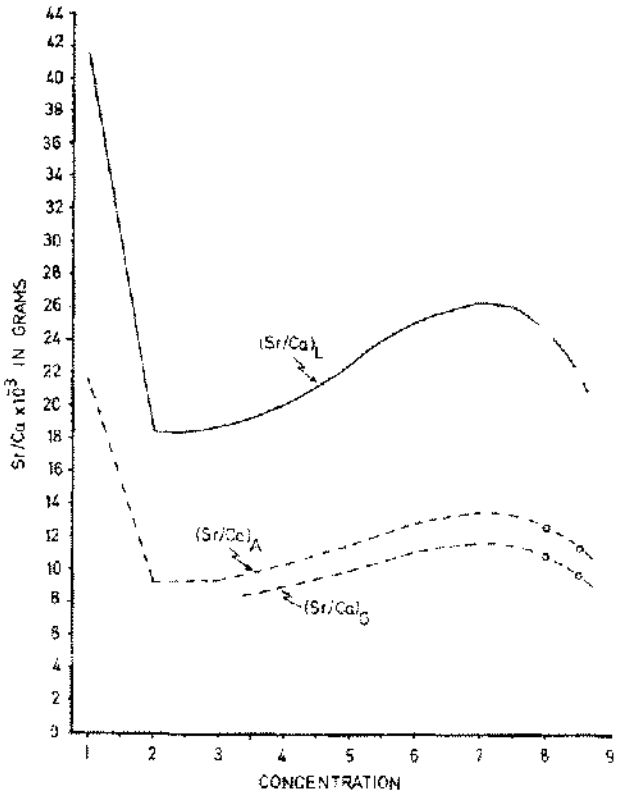

Figure 22. Sr/Ca ratios. $(Sr/Ca)_L$ = lagoon waters and sabkha brines, $(Sr/Ca)_A$ = aragonite and anhydrite, $(Sr/Ca)_G$ = gypsum.

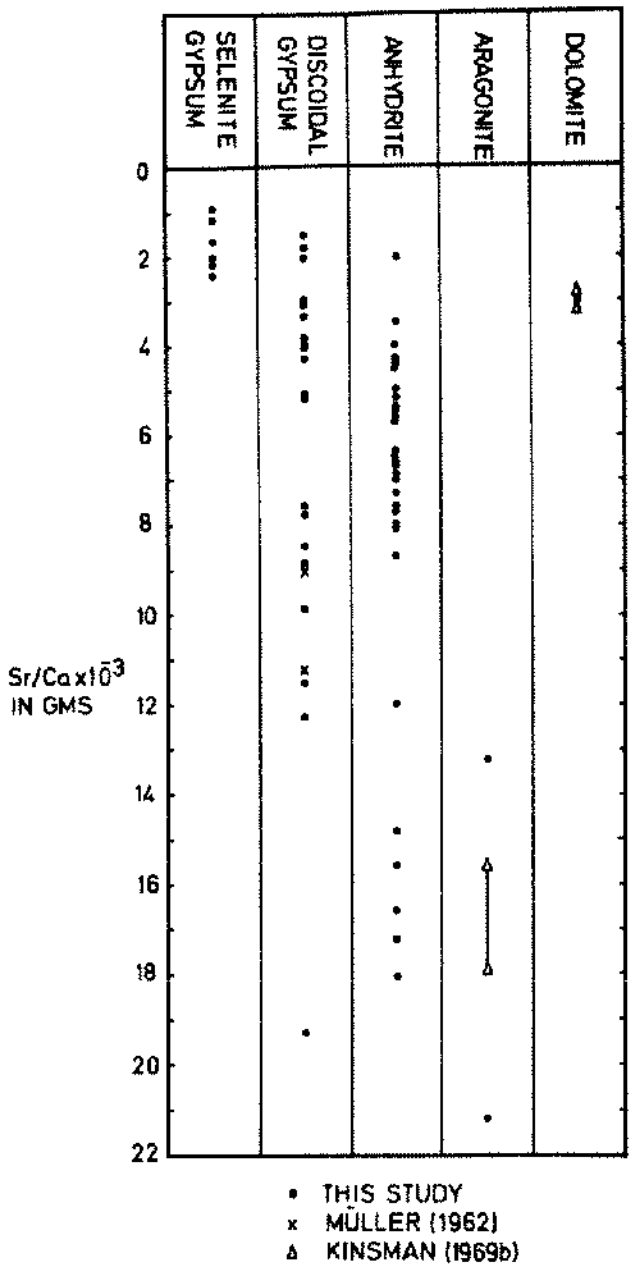

Figure 23. Sr/Ca ratios in evaporite minerals.

gypsum mush at the seaward sabkha margin are considered of very early diagenetic origin.

Observed values of $< 6\times10^{-3}$ Sr/Ca for large discoidal crystals are much lower than the predicted range of Sr/Ca for gypsum precipitated between concentrations $\times 3.35$ and $\times 7.5$, as well as from NaCl saturated brines (Fig. 22). The same problem also applies to selenite gypsum, with Sr/Ca ratios between 0.90×10^{-3} and 2.46×10^{-3}. On the basis of occurrence in the sabkha, selenite is late di genetic, and normally associated with brines sat rated with NaCl. It has been assumed as a workin hypothesis that k_{Sr} gypsum is a constant in brine of variable concentration. Although this assump tion appears to hold for gypsum crystallizing fro brines of moderate concentration, it is unlikely t hold at very high brine concentrations. Observe values of Sr/Ca ratios in large discoidal gypsu crystals and selenite crystals are attributed to a re atively small value for k_{Sr} gypsum, in the order < 0.1 in brines of concentrations $> \times 8$. In th gypsum mush at the seaward sabkha margin, sma (< 0.5mm diameter) discoidal crystals make u ≤ 20% of the mush; the larger crystals show su face textures indicative of overgrowth. Thus the is the distinct possibility that some small crysta have equilibrated with brines of increasing concer tration leading to solution and reprecipitation c small crystals to form larger crystals.

Gypsum associated with protodolomite contain an abnormally high Sr concentration. One sampl analyzed contained 0.440 wt percent Sr c 19.3×10^{-3} Sr/Ca. The associated protodolomit contained 0.066 wt percent Sr or 3.04×10^{-3} Sr/C Kinsman (1969b, p. 853) recorded values of b tween 0.06 and 0.07 wt percent Sr (Sr/Ca 2.8×10^{-3} to 3.2×10^{-3}) for protodolomite fro the sabkha.

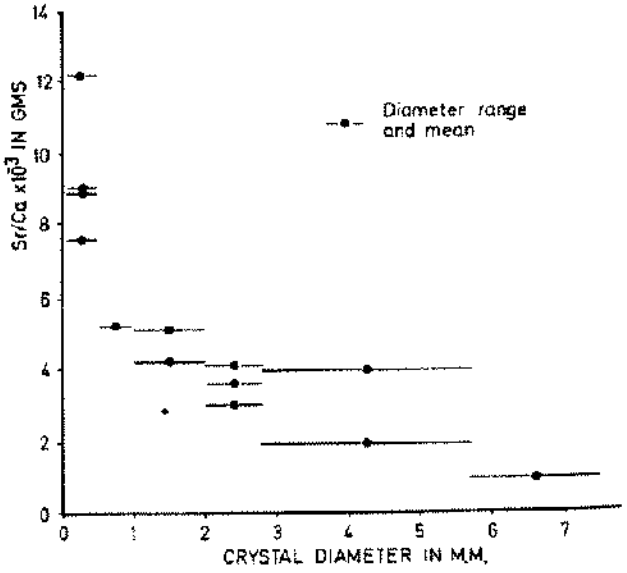

Figure 24. Correlation between Sr/Ca in discoid gypsum crystal si fractions.

The gypsum associated with protodolomite may have formed either by direct replacement of aragonite, or as a by-product of dolomitization. Assuming that the original aragonite contained 0.75 wt percent Sr (average of recorded values), and protodolomite 0.066 wt percent Sr, a simple calculation shows that 1 mol of aragonite would contain 0.0086 m.mol Sr, and 1 mol protodolomite, 0.0003 m.mol Sr. The established relationship for dolomitization is:

2 mol Aragonite = 1 mol Protodolomite + 1 mol Gypsum.

The mineral assemblage coexisted with brine of concentration ×8.2. The maximum amount of Sr which such a brine could contain based on the solubility product of celestite is approximately 0.015 m.mol (Fig. 21). A mass balance of Sr based on the aragonite-protodolomite relationship and allowing for the amount of Sr depleted by celestite crystallization, indicates that 1 mol of gypsum formed as a by-product of the reaction should contain about 0.0025 m.mol Sr or about 0.37 wt percent Sr. This value approximately agrees with the observed Sr in the gypsum of 0.44 wt percent Sr (0.003 m.mol Sr), which is consistent with the origin of this gypsum dominantly as a by-product of dolomitization.

In summary, there is tentative correlation of Sr concentration in gypsum crystals in the sabkha with brine evolution and dolomitization. Further, the data reflect several generations of crystals precipitated from the brines, and distinguishes between early and late diagenetic gypsum.

Anhydrite. Strontium in anhydrite ranges from 0.127 to 0.50 wt percent Sr ($Sr/Ca = 3.5\times10^{-3}$ to 18×10^{-3}). Most of the values fall between 0.127 and 0.260 wt percent Sr ($Sr/Ca = 3.5\times10^{-3}$ to 8.85×10^{-3}) (Fig. 23).

Anhydrite first occurs at the seaward sabkha margin, in association with gypsum, in contact with brines of concentrations about ×7.5. If this anhydrite is a primary precipitate, it should have a maximum Sr/Ca ratio of about 13×10^{-3} (Fig. 22). At concentrations > ×7.5 Sr/Ca, if the distribution coefficient is < 0.50, values should be $< 13\times10^{-3}$ or $\ll 13\times10^{-3}$ owing to the probable effects of high brine concentration on the distribution coefficient. Similar values would also be obtained if gypsum reacted with brines at concentration ×7.5. If this were the case, then Sr/Ca (anhydrite) should exceed Sr/Ca (gypsum) by about 15 percent if the reaction takes place at concentration ×7.5. At concentrations > ×7.5 this difference may be < 15 or > 15 percent depending on the relative changes in the distribution coefficients. It is of note that the average Sr/Ca ratio differs by about +13 percent in coexisting supratidal gypsum and anhydrite in the Gulf of California (Butler, 1970). These minerals are closely associated with brines of an average concentration of approximately ×7.5.

Large (about 50 gm) initial samples of gypsum and anhydrite were used in the analysis for Sr. These data will consequently reflect various stages in the diagenetic evolution of gypsum and anhydrite. For example, if a sample was of anhydrite formed from a mush of gypsum in which the ratio of large discoidal (late diagenetic) to small discoidal (early diagenetic) crystals was variable, the Sr/Ca in anhydrite samples analyzed would reflect this variation. A high proportion of large gypsum crystals would yield a relatively small total Sr/Ca (gypsum) and consequently a relatively small total Sr/Ca (anhydrite). The converse would apply if there were a high proportion of small gypsum crystals. If in addition, some crystals in the anhydrite sample were formed as a primary precipitate or by replacement of aragonite, the Sr/Ca in the anhydrite sample would be further modified depending on the size of the contribution to the sample of crystals of these diverse origins.

Weighed size fractions of samples of gypsum crystals from the surface gypsum mush at the seaward sabkha margin were analyzed for Sr. The samples contained an average of approximately 0.12 wt percent Sr, or 5.0×10^{-3} Sr/Ca. Strontium concentrations and Sr/Ca ratios in anhydrite samples from essentially aragonite free horizons in the sabkha are summarized as follows:

Location/Type	No. Samples	av. wt percent Sr	av. Sr/Ca
Nodules (isolated)	9	0.130	5.6×10^{-3}
Upper portion of secondary anhydrite seam	13	0.140	6.0×10^{-3}

If these anhydrites formed from gypsum crystals with an average Sr/Cr ratio of approximately 5×10^{-3}, values of Sr/Ca in secondary anhydrites should be greater than that in the parent gypsum by about 15 percent. In fact, the average Sr/Ca in samples of anhydrite nodules and anhydrite from the upper portion of the major anhydrite seam in

the mid-sabkha region (which is the lateral stratigraphic equivalent of the surface gypsum mush at the seaward sabkha margin) differs from Sr/Ca = 5×10^{-3} by between +10 percent and +20 percent. Consequently, the observed spread in the Sr/Ca ratio in most of the anhydrite samples from 3.5×10^{-3} to about 8×10^{-3} (Fig. 23) could be attributed to an initial range in the ratio of large to small discoidal gypsum crystals in the original parent gypsum crystal.

Naturally, the foregoing correlations do not prove that the bulk of the samples of anhydrite analyzed originated by alteration of metastable gypsum, but the close degree of Sr data correlation, together with the observed stratigraphic and textural relationships between gypsum and anhydrite in the sabkha, are consistent with this hypothesis.

A further problem concerns the interpretation of anhydrite samples with Sr/Ca ratios ranging from between about 12×10^{-3} and 18×10^{-3} (Fig. 23). These samples were taken from the lower portion of the major anhydrite seam in the mid-sabkha region, immediately above the subsurface algal mat. These anhydrites occurred in association with aragonite and a trace of diagenetic protodolomite. Multiple sample analysis, and technique of sample preparation for analysis, preclude contamination with celestite. The origin of anhydrite crystals in these samples may be attributed to one, or a combination of the following processes: (1) primary precipitation, (2) direct replacement of aragonite, and/or (3) alteration of a mush of gypsum crystals in which the ratio of large to small discoidal gypsum crystals was very small.

In order to obtain such large values of Sr/Ca for anhydrite from small gypsum crystals, the parent samples of gypsum would have had to be composed totally of very small crystals. Such a situation has not been observed in the surface gypsum mush at the seaward sabkha margin. In aragonite, Sr/Ca ratios range between about 13×10^{-3} and 19×10^{-3}. If aragonite were replaced by anhydrite, the anhydrite should also have the same range of Sr/Ca values since the distribution coefficients have about the same values. Thus some anhydrite in the sabkha may have originated by equilibration of aragonite with brines.

Secondary gypsum from Facies 5 contains less Sr than the parent anhydrite. Secondary gypsum crystals contain between 0.032 and 0.048 wt percent Sr, with an average for three samples of 0.041 wt percent Sr (Sr/Ca = 1.38×10^{-3} to 2.07×10^{-3}; av. 1.76×10^{-3} Sr/Ca). The parent anhydrites contain approximately 0.127 wt percent Sr, or 4.33×10^{-3} Sr/Ca. These data, together with the observed association of anhydrite and celestite at gypsum crystals boundaries, is consistent with a solution-precipitation process for the anhydrite to gypsum conversion. The Sr released by the reaction of anhydrite with brines is precipitated as celestite.

ANHYDRITE STRUCTURES

Most of the structures so far reported in ancient calcium sulphate sequences occur in the sabkha. These structures include enterolithic anhydrite seams, polygonal layers, plicated seams, overthrust folds, and diapir-like features amongst others. Some structures appear to be the result of combined processes of anhydrite growth, slumping, and compaction, and some structures are inherent from the supratidal origin of anhydrite.

Polygonal anhydrite layers.

Polygonal anhydrite layers, festooned in cross-section, are a consequence of anhydrite development within a supratidal environment. Anhydrite first occurs at the landward surface of the gypsum mush (Facies 2) as isolated blebs and small nodules. Traced inland, nodules show an increase in size and number to eventually form a surface layer of interlocking polygons. Further inland, where this layer becomes progressively overlain by recycled aeolianite, the polygons are festooned in section and range in diameter from about 30 cm to 1.5 m. Additional polygons may be built up within an original anhydrite polygon. The upturned limbs of polygons are characteristically planed off (Figs. 15c, 25b). Erosion surfaces are common within the upper 30 cm of supratidal sediment and reflect past episodic flooding of the sabkha surface. Slumping and compaction, due to alteration of the immediately underlying gypsum mush to anhydrite as well as continued growth of polygons, locally distorts the originally symmetrical layering of some polygons (Fig. 25b). Subsequent development of some anhydrite structures further inland, in the mid-sabkha region, are to some extent influenced by these polygonal anhydrite layers.

Diapir-like features.

Features in anhydrite which resemble diapirs develop from the seam of secondary anhydrite overlying the subsurface algal mat in the mid-sabkha region (Facies 4). In some localities they are essentially deformational features, formed as a consequence of the original gypsum mush occurring between adjacent limbs of anhydrite polygons. The

diapir-like shape has been enhanced by slumping and growth of polygons (Fig. 25b).

In other localities they appear to have formed as true piercement structures (Fig. 25c). A hiatus, characterized by a thin seam of nodular anhydrite, commonly occurs at the top of these diapirs (Fig. 25d). These piercement structures are restricted in the sabkha to the vicinity south and east of Bougeba, an area in which the groundwaters are of continental or of mixed marine and continental origin. Thus it is likely that the piercement structures are the result of influx of continental groundwaters which have supplied components for additional anhydrite growth.

Similar diapir-like features have been reported from the Miocene Fars of Iraq (N. Falcon, in a discussion at the Geological Society, London, 1965) and from the English Purbeckian (D.J. Shearman, personal communication, 1969).

Contorted and folded seams.

Contorted and folded anhydrite seams occur through Facies 4. Contorted anhydrite seams, which in vertical section resemble convolutions of intestines, have been termed "enterolithic veins" (Hahn, 1912). In the sabkha, contorted seams frequently occur within the upper 30 cm of recycled aeolianite (Fig. 26a). Similar structures have been described by West (1964, Plate 3, Figs. 5, 6) from the Purbeckian of southern England, and Holliday (1965) from the Carboniferous of Spitsbergen.

Examples of folded anhydrite seams from the sabkha are shown in Figures 27 and 26b, 15e, 25d).

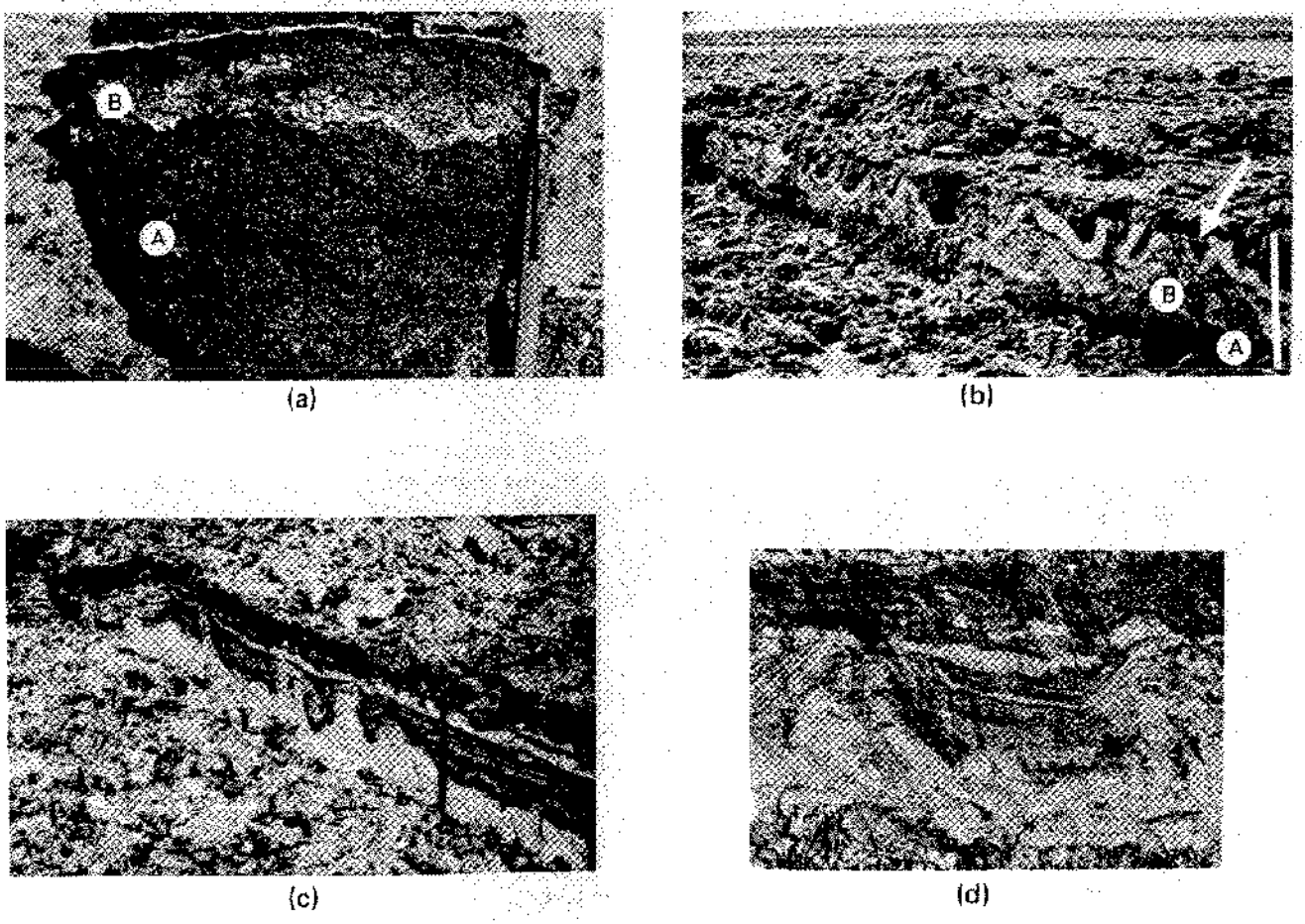

Figure 25.(a) Nodular anhydrite from the Gulf of California. A = gypsum + detrital sediment, B = anhydrite + gypsum + detrital sediment. Pencil as scale = 9 cm; (b) Contorted anhydrite festoons. A = gypsum mush, B = anhydrite (A+B = original gypsum mush). Note (i) incipient diapir-like feature above B, and (ii) an erosion surface. Scale = 30 cm; (c) Diapirs stemming from the top of the seam of secondary anhydrite. Note collapse structures between adjacent diapirs. Machete as scale = 0.6 m; (d) Hiatus at top of diapirs (left). Note plications in thin anhydrite seams between diapirs. Scale (left) = 15 cm.

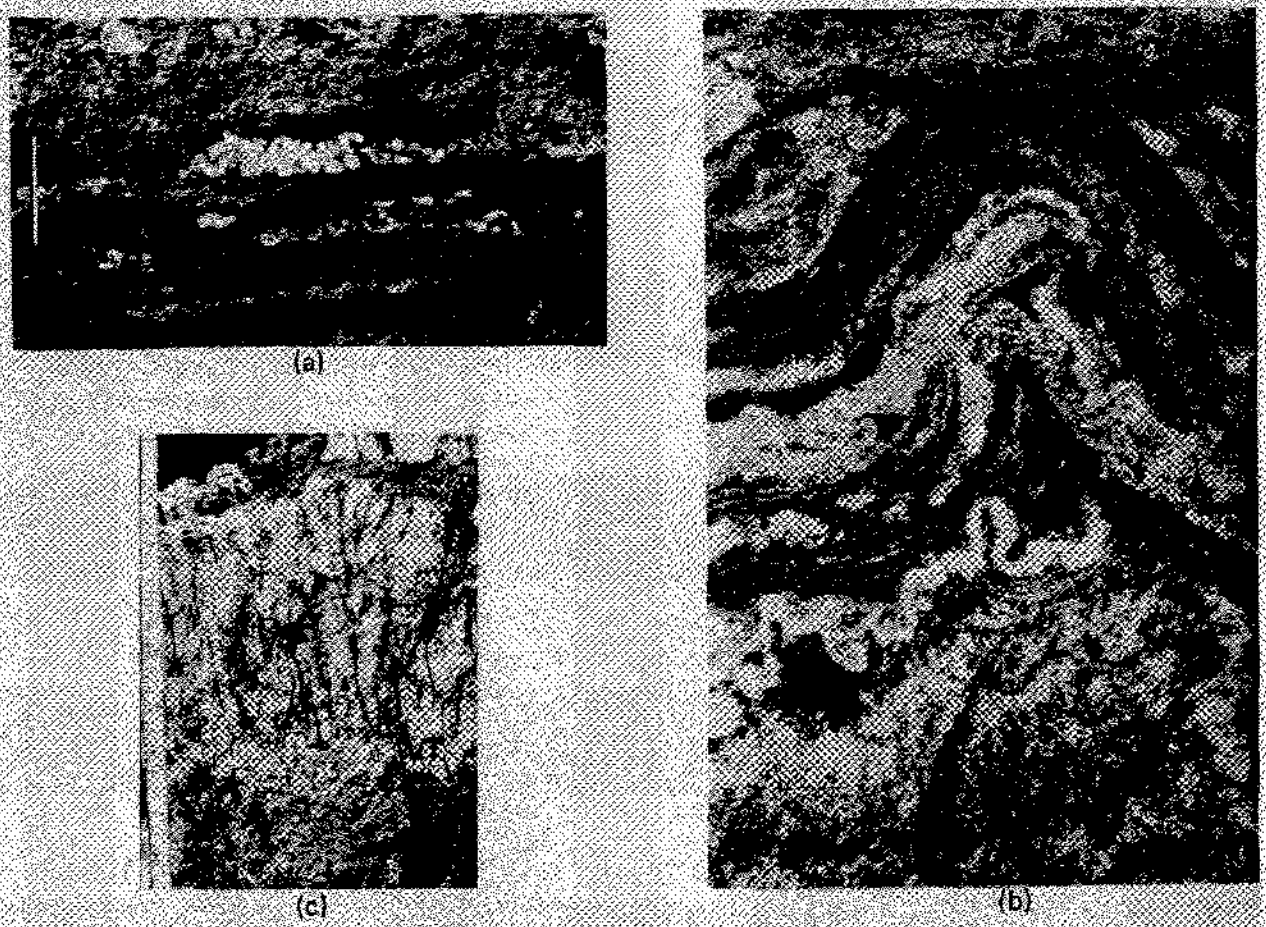

Figure 26. (a) Enterolithic anhydrite seam in recycled aeolianite. Scale = 8 cm; (b) Enlargement of the overthrust fold shown in F (right). Note hiatus 4 cm from top; (c) Vertical sand veins in nodular anhydrite.

Figure 27. Anhydrite structures in recycled aeolianite overlying algal laminae. Note (i) plications in anhydrite seams, (ii) collapse struc (iii) anhydrite layer showing brittle fracture (center), (iv) overthrust fold (right). Scale = 20 cm.

Sand veins.

Vertical sand veins which resemble worm tubes are common in nodular anhydrite, in anhydrite seams developed throughout the sabkha, but predominate in seams occurring at the inland margin of Facies 4 and in Facies 5 (Fig. 26c). These veins originate in the low supratidal, water saturated gypsum mush. Organisms to which these veins could be attributed were not observed in the gypsum mush. Apparently the sand veins have formed by a physical process. They may have formed in this environment either by settling convection (Kuenen, 1968) or by flooding. Surface floodwaters would tend to trap air in the surface sediment layers. The subsequent release of air from the sediments could give rise to vertical passages which subsequently become infilled with sediment.

Since the sand veins originated in a gypsum mush, anhydrite observed to contain these veins is secondary and formed from the alteration of gypsum. By analogue, the presence of similar vertical veins in ancient nodular anhydrites would suggest formation within a supratidal setting, and the secondary origin of the anhydrite.

Although anhydrite occurring in aeolianites at the landward sabkha margin (Facies 5) has a nodular texture, deformational structures of the types described above have not been observed. Furthermore, deformational structures do *not* occur in areas where anhydrite seams have hydrated to gypsum.

CONCLUSIONS

There are three sources of components for diagenetic evaporite minerals in a Trucial Coast supratidal flat: marine waters, continental groundwaters, and carbonate sediments. Marine waters are supplied by surface flooding. Continental groundwaters are supplied by influx laterally and vertically into sabkha sediments from surface and subsurface Pleistocene aeolianites. Evaporites are also formed by exchange reactions between brine and host sediment components. The supratidal flat (sabkha) is a weathering profile in which a variety of diagenetic processes have acted together to form evaporite facies. Distribution of these facies has been modified, with reference to diagenetic patterns which would normally be produced solely by marine connate brines, by input of components from continental groundwaters. The seaward accretion of the sabkha profile is accompanied by three diagenetic environments. An environment of active diagenesis is located at the seaward margin, and an in part retrogressive diagenetic environment at the landward margin. In the mid-sabkha environment, equilibrium appears to have been reached between brines and host evaporite-carbonate sediments, except where there is local overlap of the continental groundwater environment onto the normal marine water diagenetic environment. Local continued growth of anhydrite seams resulting in the formation of structures, has resulted from the mixing of these brines in the mid-sabkha environment. In short, the sabkha constitutes a dynamic diagenetic system with a variety and complex assemblage of evaporite facies.

Combined trace element data, stratigraphic and textural relationships between aragonite, gypsum, anhydrite and protodolomite, and brine chemistry are broadly consistent with the following origins for some species of evaporite minerals in the sabkha:

(1) Origin of gypsum:
  (a) Primary precipitate.
  (b) Replacement of aragonite.
  (c) Replacement of aragonite via dolomitization process.
  (d) Hydration of anhydrite.

(2) Origin of anhydrite:
  (a) Replacement of primary gypsum.
  (b) Replacement of aragonite.
  (c) Replacement of gypsum formed as a by-product of dolomitization(?).
  (d) By-product of dolomitization, but not via intermediary gypsum(?).

(3) Origin of protodolomite: Reaction of Mg in brines with host aragonite sediments, by the reaction:

$$2\,CaCO_3 + Mg = MgCa(CO_3)_2 + Ca.$$

The data suggest that the process of gypsum dehydration to anhydrite is essentially a solution-precipitation process. Both the alteration of aragonite to anhydrite to gypsum also appear to be processes of solution-precipitation. The nodular texture of anhydrite is the result of initial formation of anhydrite from gypsum.

Finally, there is the problem of primary anhydrite in the sabkha. Stratigraphic and textural relationships, and the geochemical data, appear consistent with an origin of anhydrite from processes other than primary precipitation. A primary origin for some anhydrite in the sabkha on a

micro-scale, cannot be completely ruled out. It is concluded, however, that if some primary anhydrite does occur, it is volumetrically insignificant to anhydrite formed from other processes, particularly from the alteration of gypsum.

ACKNOWLEDGEMENTS

This paper is based on work done at Imperial College, London, and the University of California at Riverside. The late Department of Scientific and Industrial Research (U.K.) and the Dry Lands Research Institute (U.C. Riverside) provided financial support. The writer thanks those who have generously given advice and assistance: Lewis Cohen, Frank Dickson, Christopher Kendall, Ray Murray, Perry Roehl, and Douglas Shearman.

REFERENCES

Arons, A.B., and Kientzler, C.F., 1954, Vapour pressure of sea-salt solutions: Am. Geophys. Union Trans. v. 35, p. 722-728.

Butler, G.P., 1965, Early diagenesis in the Recent sediments of the Trucial Coast of the Persian Gulf: Unpub. M.Sc. Thesis, Univ. London, 251 p.

——, 1969a, Modern evaporite deposition and geochemistry of coexisting brines, the sabkha, Trucial Coast, Arabian Gulf: Jour. Sedimentary Petrology, v. 39, p. 70-89.

——, 1969b, Interpretation of strontium concentrations in Holocene and ancient evaporite minerals, (in press).

——, 1970, Secondary anhydrite from a sabkha, North West Gulf of California, Mexico, *in* symposium on salt: Northern Ohio Geol. Soc., (this volume).

Cayeux, L., 1935, Les roches sedimentaires de France—Roches Carbonatees: Masson et Cie, Paris.

Curtis, R., Evans, G., Kinsman, D.J.J., and Shearman, D., 1963, Association of dolomite and anhydrite in the Recent sediment of the Persian Gulf: Nature, v. 197, p. 679-680.

Deffeyes, K.S., Lucia, F.J., and Weyl, P.K., 1965, Dolomitization of Recent and Plio-Pleistocene sediments by marine evaporite waters on Bonaire, Netherlands Antilles, *in* Dolomitization and limestone diagenesis. A symposium: Soc. Econ. Paleontologists and Mineralogists Spec. Pub. 13, p. 71-88.

Evans, G., 1965, Intertidal flat sediments and the environment of deposition in the Wash: Geo Soc. London Quart. Jour., v. 121, p. 209-247.

——, Kendall, C.G. St. C., and Skipwith, Sir Pa rick A. d'E., 1964, Origin of the coastal flat the sabkha, of the Trucial Coast, Persi Gulf: Nature, no. 202, p. 759-761.

Fuller, J.G.C.M., and Porter, J.W., 1969, Evapori formation with petroleum reservoirs in Devoni and Mississippian of Alberta, Saskatchewan, ar North Dakota: Am Assoc. Petroleum Geologis Bull., v. 53, p. 909-926.

Hahn, F.F., 1912. Untermeerische Gleitung b Trenton Falls (Nordamerika) und ihr Verhaltn zu ahnlichen Storungsbildern: Neues Jahr Mineralogie Geologie Palaontologie, v. 36, 1-41.

Hardie, L.A., 1967, The gypsum-anhydrite equili rium at one atmosphere pressure: Am. Minera ogist, v. 52, p. 171-200.

Holliday, D.W., 1968, Early diagenesis of Midd Carboniferous nodular anhydrite of Spitsbe gen: York. Geol. Soc. Proc., v. 36, p. 277-29

Holser, W.T., 1966, Diagenetic polyhalite in R cent salt from Baja California: Am. Mineral gist, v. 51, p. 99-109.

Illing, L.V., Wells, A.J., and Taylor, J.C.M., 196 Penecontemporary dolomite in the Persian Gul *in* Dolomitization and limestone diagenesis. symposium: Soc. Econ. Paleontologists an Mineralogists Spec. Pub. p. 89-111.

Kendall, C.G.St.C., and Skipwith, Sir Patrick A d'E., 1968, Recent algal mats of a Persian Gul Lagoon: Jour. Sed. Petrology, v. 38, 1040-1058.

——, and——, 1969, Geomorphology of a Recen shallow-water carbonate Province: Khor Bazam, Trucial Coast, southwestern Persia Gulf: Geol. Soc. Am. Bull., v. 80, p. 865-892

Kerr, S.D., and Thompson, A., 1963, Origin o nodular and bedded anhydrite in Permian shel sediments, Texas and New Mexico: Am. Assoc Petroleum Geologists Bull., v. 47, p. 1726-1732

King, P.B., 1942, Permian of west Texas and south eastern New Mexico: Am. Assoc. Petroleum Geologists Bull., v. 26, p. 535-763.

Kinsman, D.J.J., 1964, Recent carbonate sedi mentation near Abu Dhabi, Trucial Coast

Persian Gulf: Unpub. Ph.D. Dissertation, Univ. London, 302 p.

——, 1966, Gypsum and anhydrite of Recent age, Trucial Coast, Persian Gulf, *in* Second symposium on salt, v. 1: Northern Ohio Geol. Soc., p. 302-306.

——, 1969a, Early diagenesis of carbonate sediments in a supratidal setting: Am. Petrol. Inst. Semi-Annual Progress Report (January), 10 p.

——, 1969b, Modes of formation, sedimentary associations, and diagenetic features of shallow water and supratidal evaporites: Am. Assoc. Petroleum Geologists Bull., v. 53, p. 830-840.

——, and Holland, H.D., 1969, The coprecipitation of cations with $CaCO_3$-IV. The coprecipitation of Sr^{2+} with aragonite between 16° and 96°C: Geochem. Cosmochim. Acta, v. 33, p. 1-17.

Klement, M.C., 1895, Sul l'origine de la dolomie dans les formations sedimentaires: Bull. Soc. Belge., v. 9, Mem. 3, p. 23.

Kuenen, PH. H., 1968, Settling convection and grain size analysis: Jour. Sed. Petrology, v. 38, p. 822.

Lucia, F.J., 1968, Recent sediments and diagenesis of south Bonaire, Netherlands Antilles: Jour. Sedimentary Petrology, v. 38, p. 845-858.

Masson, P.H., 1955, An occurrence of gypsum in southwest Texas: Jour. Sed. Petrology, v. 25, p. 72-77.

Miller, D.N., 1961, Early diagenetic dolomite associated with salt extraction process, Inagua, Bahamas: Jour. Sed. Petrology, v. 31, p. 473-476.

Mojola, R.J., and Glover, E.D., 1965, Recent anhydrite from Clayton Playa, Nevada: Am. Mineralogist, v. 50, p. 2063-2069.

Muller, G., and Puchelt, H., 1961, Die Bildung von Colestin ($SrSO_4$) aus Meerwasser: Naturw, v. 48, p. 301-302.

——, 1962, Zur Geochemie des Strontiums in ozeanen Evaporiten unter besonderer Berucksichtigung der sedimentaren Coelestin lagerstatte von Hemmelte-West (Sud-Oldenburg): Geologies, Beiheft 35, p. 1-90.

Murray, R.C., 1964, Origin and diagenesis of gypsum and anhydrite: Jour. Sed. Petrology, v. 34, p. 512-523.

Philips, F.C., 1947, Oceanic salt deposits: Chem. Soc. Quart. Rev., v. 1, p. 91-111.

Phleger, F.B., and Ewing, G.C., 1962, Sedimentology and oceanography of coastal lagoons in Baja California, Mexico: Geol. Soc. America Bull., v. 73, p. 145-182.

——, 1969, Modern evaporite deposit in Mexico: Am. Assoc. Petroleum Geologists Bull., v. 53, p. 824-829.

Posnjak, E., 1940, Deposition of calcium sulphate from seawater: Am. Jour. Sci., v. 238, p. 559-568.

Price, W.A., 1955, Environment and formation of the chenier plain: Texas A. and M. Res. Found. Project 63, Ref. 54-64T.

Privett, D.W., 1959, Monthly charts of evaporation from the North Indian Ocean (including the Red Sea and the Persian Gulf): Royal Meteorol. Soc. Quart. Jour., no. 85, p. 424-428.

Purkayastha, B.C., and Chatterjee, A., 1966, The study of the uptake of strontium tracer by different forms of calcium sulphate: Jour. Indian Chem. Soc., v. 43, p. 687-693.

Riley, C.M., and Byrne, J.V., 1961, Genesis of primary structures in anhydrite: Jour. Sed. Petrology, v. 31, p. 553-559.

Rooney, L.F., and French, R.R., 1968, Allogenic quartz and the origin of penemosaic texture in evaporites of the Detroit River Formation (Middle Devonian) in northern Indiana: Jour. Sed. Petrology, v. 38, p. 755-765.

Shearman, D.J., 1966, Origin of marine evaporites by diagenesis: Inst. Mining Metallurgy (Newcastle-upon-Tyne) Trans. Sec. B., v. 75, p. 208-215.

Shinn E.A., Ginsburg, R.N., and Lloyd, R.M., 1965, Recent supratidal dolomite from Andros Island, Bahamas, *in* Dolomitization and limestone diagenesis. A symposium, Soc. Econ. Paleontologists and Mineralogists Spec. Pub. 13, p. 89-111.

Stewart, F.H., 1963, Marine evaporites. Chapter Y *in* Data of geochemistry, 6th ed., U.S. Geol. Surv. Prof. paper 440-Y, p. 40.

Walker, T.R., and Thompson, R.W., 1968, Late Quaternary geology of the San Felipe area, Baja California, Mexico: Jour. Geology, v. 76, p. 479-485.

Wells, A.J., 1962, Recent dolomite in the Persian Gulf: Nature, v. 194, p. 274-275.

West, I.M., 1965, Macrocell structure and enterolithic veins in British Purbeck gypsum and anhydrite: York, Geol. Soc. Proc., v. 35, p. 47-58.

Wood, E.J.F., 1962, The microbiology of estuaries *in* The environmental chemistry of Marine Sediments. A symposium: Univ. Rhode Island, Occ. Pub. 1, p. 20-26.

Zen, E-AN, 1965, Solubility measurements in the system $CaSO_4$-NaCl-H_2O at 35°, 50° and 70° and one atmosphere pressure: Jour. Petrology v. 6, p. 124-164.